Analysis of genetic interaction between the cAMP/PKA pathway and the EB1 family protein Mal3 in *Schizosaccharomyces pombe*

(分裂酵母 cAMP/PKA 経路と EB1 ファミリータンパク質 Mal3 の遺伝学的関連性の解析)

Takuma Tanabe

2020

Table of Contents

Abbreviations

APC	anaphase-promoting complex
ATP	adenosine triphosphate
cAMP	cyclic adenosine monophosphate
CH	calponin homology
EB1	end-binding 1
EMM	Edinburgh minimal medium
FACS	fluorescence-activated cell sorting
GFP	green fluorescent protein
LatA	latrunculin A
MAPs	microtubule associated proteins
MBC	methyl-2-benzimidazole carbamate
mRFP	monomeric red fluorescent protein
MTOC	microtubule organization center
NBRP	National Bio Resource Project
PKA	protein kinase A
SAC	spindle assembly checkpoint
SPB	spindle pole body
TBZ	thiabendazole

Chapter 1

General introduction

Fission yeast

A fission yeast *Schizosaccharomyces pombe* is a rod shaped unicellular eukaryote, of which cell size is 7-14 μm in length and ~4 μm in width. *S. pombe* has been used as a model organism for investigating basic cellular mechanisms through genetics and molecular biology, and also applied to bio-production of foreign proteins or beneficial compounds [1]. *S. pombe* genome consists of three chromosomes of 5.7Mb, 4.6Mb, and 3.5Mb, which encode 5,118 proteins in total [2].

Life cycle and cell cycle in fission yeast

S. pombe grows in both haploid and diploid states, while haploid is more stable. *S. pombe* goes through a typical eukaryotic cell cycle consisting of the G1, S, G2, and M phases in the mitotic growth phase (Fig. 1-1A and [3]). However, when the cells are shifted to a nutrient restricted condition, they proceed the sexual differentiation process; opposite mating type (h^- and h^+) cells conjugate and proceed meiosis to generate haploid four spores. If nutrient condition is restored at the point after mating, the cells enter the mitotic cycle to form diploids, and if it is happened after sporulation, the cells naturally grow by haploids (Fig. 1-1).

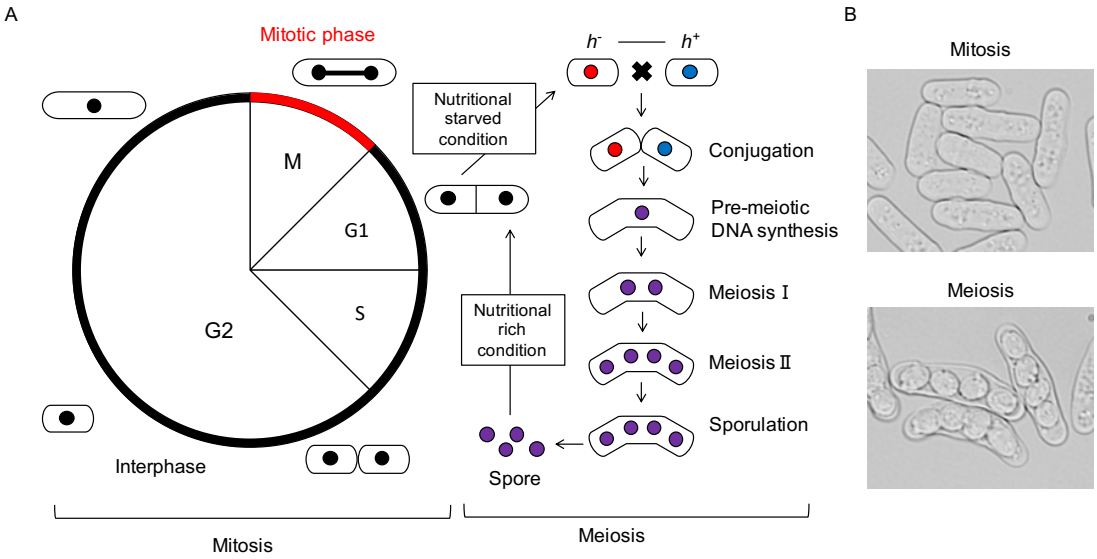

Fig. 1-1 The life cycle of *S. pombe*

(A) A life cycle of haploid mitotic cell cycle (left), and sexual differentiation process in meiosis (right). Under nutrient rich condition, *S. pombe* haploid cells proliferate through mitotic cell cycle. However, when nutrient is starved, *S. pombe* undergoes sexual differentiation process with opposite mating type, and make four spores. Spores start mitotic cell cycle when nutrients are sufficient (B) A bright field image in mitosis (top) and sporulation of meiosis (bottom)

Mitotic phase

Each pair of chromosomes is separated to two identical and independent chromosomes during mitosis, which consists of five stages including prophase, prometaphase, metaphase, anaphase, and telophase (Fig. 1-2). In prophase, interphase microtubules in cells disappeared and condensed chromosomes are formed. In prometaphase, cells form bipolar spindle pole bodies (SPBs), which are similar in the function of mammalian centrosomes. In metaphase, microtubules adhere to kinetochore which are monitored by the spindle assembly checkpoint (SAC). If a mistake is made in this attachment, anaphase-promoting complex (APC) is activated, thereby preventing progression of metaphase to anaphase until the proper attachment is resumed. Sister chromosomes are segregated by SPB during anaphase A and spindle elongation occurs during anaphase B. In telophase, cells disassemble spindles, re-orientate interphase microtubules, form septum, and proceed to cytokinesis.

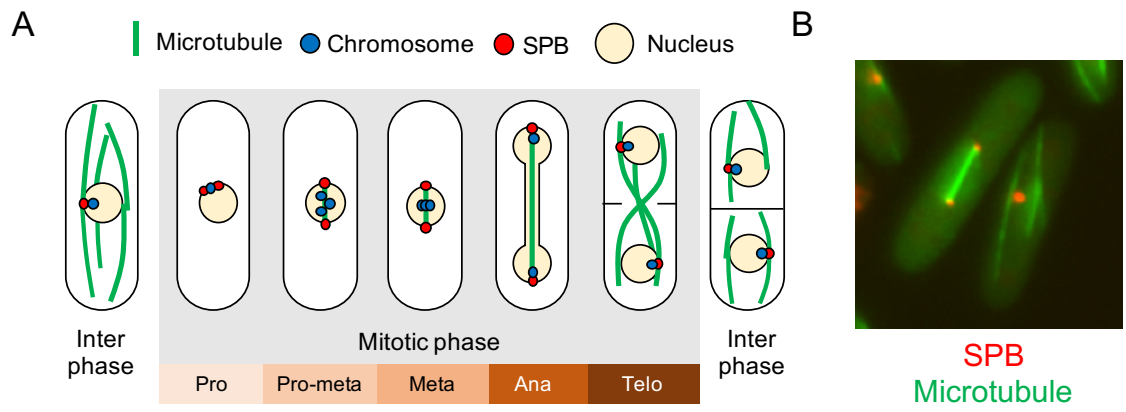

Fig. 1-2 Distribution of microtubules, chromosomes, and SPB during mitosis

(A) In interphase, microtubules (green) organizes 3-4 bundles and locate along the long axis. SPB (red) binds to the kinetochore of chromosomes (blue). In prophase, interphase microtubules disappear and short spindles are formed from one SPB to another SPB. In pro-metaphase, cells form bipolar spindle and oscillate sister-chromosomes. In metaphase, sister-chromosomes are aligned at the center. In anaphase, spindle elongates and sister-chromosomes are segregated. In telophase, cells disassemble the spindle, reorient interphase microtubule, form septum and proceed to cytokinesis. (B) Visualization of SPB and microtubules in *S. pombe* cells. SPBs are visualized by Sad1-mRFP, which is the fusion of a component of SPB. Microtubules are visualized by GFP-Atb2, which is a fusion of the component of α-tubulin.

Microtubules and microtubule associated proteins

Microtubules are the major cytoskeletal fibers in eukaryotic cells, and their localization is arranged along the long axis of cells. Microtubules regulate material transport, cell shape formation, and chromosome segregation. Microtubules are assembled into head to tail to form polar 13 protofilaments consisting of tubulin polymers, which are made up of heterodimer of α-tubulin and ß-tubulin. Microtubule protofilaments are polarized with the minus end that expose α-tubulin, and the plus end that expose β-tubulin. Normally, microtubule minus ends are anchored in microtubule organizing centers (MTOC), which consist of γ-

tubulin and γ-tubulin associated proteins. On the other hand, the plus end switches between growing and shrinking phases through rescue and catastrophe events, known as dynamic instability [4]. The dynamic instability on the plus end is based on binding and hydrolysis GTP at the nucleotide exchangeable site of β-tubulin. The dynamic instability is regulated by microtubule associated proteins (MAPs). Especially, the plus end tracking protein (+TIP), such as XMAP215, EB1, CLIP170, and CLASP1, has a pivotal role [5,6]. Fission yeast has two α-tubulins (Nda2 and Atb2) [7], one ß-tubulin (Nda3) [8], and one γ-tubulin (Gtb1) [9,10]. In fission yeast, interphase microtubules extend along the long axis of cell, and mitotic microtubules (spindle) form the liner structure to both poles. [6].

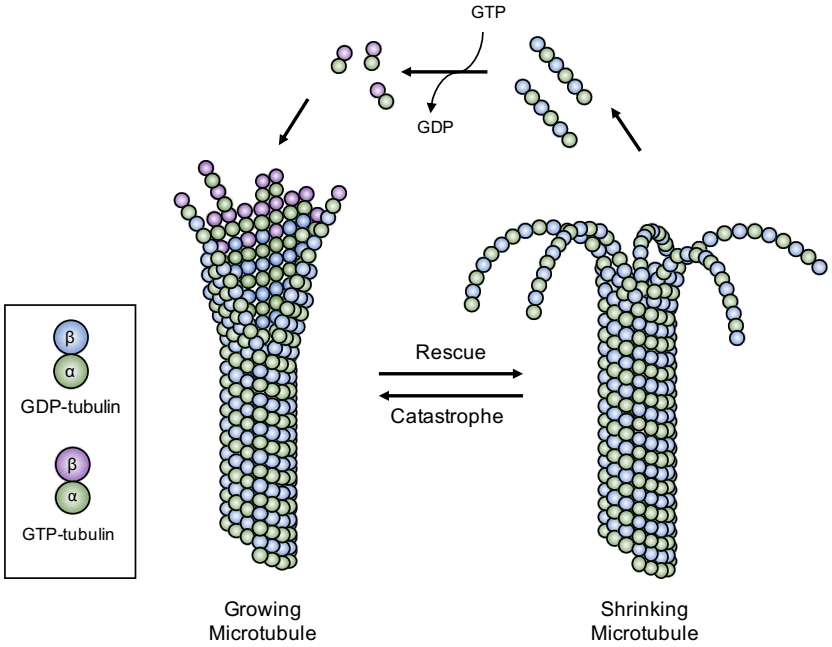

Fig.1-3 Microtubule structure and dynamic instability

The growing microtubule is polymerized with GTP type tubulin hetero dimer at the plus end. The incorporated GTP-tubulin is subsequently hydrolyzed, thus GTP-type tubulin is found only at the microtubule growing end. This structure is called "cap", and this structure promotes the elongation of microtubules. Loss of this structure causes microtubule collapse and caused microtubules shrinking. Switching between microtubule extension and shortening is called 'Rescue', and switching from shortening to extension is called 'Catastrophe'.

Kinesin

Kinesin is a type of ATP-dependent motor proteins that moves along microtubules. There are three major groups of kinesins classified according to the position of motor domain; N-terminal kinesins, middle kinesins, and C-terminal kinesins [11]. Fission yeast has nine types of kinesin, which include a type-5 kinesin family Cut7 and a type-14 kinesin family Pkl1/Klp2 [12]. Cut7, Pkl1 and Klp2 regulate bipolar spindle formation in mitosis. Since Cut7 is N-terminal kinesin and forms heterodimer, microtubule is crosslinking antiparallel microtubule and this motor protein moves toward the microtubule plus end [13].

Because Pkl1/Klp2 are C-terminal kinesin, these motor proteins move toward the microtubule minus end [14–16]. If the proper force is unbalanced by Cut7 and Pkl1/Klp2, cells increase the monopolar spindle [17–19].

The EB1 family protein in fission yeast

End-binding 1 protein (EB1) was first identified by genetic screening as an Adeno tumor polyposis coli (APC) protein binding partner in human [20]. EB1 is a plus-end tracking protein (+TIP) and binds to the microtubule growing end. EB1 binds with various proteins, such as CLIP170, CLASP, and XMAP215. The EB1 protein controls microtubule dynamics on the plus end for proper microtubule function. The EB1 family proteins are approximately 300 amino acid residues in length, and consists of two high conserved domains (the CH and EB1 or EBH domains), the flexible linker domain, the C-terminal coiled-coil region, and the flexible C-terminal sequence EEY/F motif [21]. The CH domain is highly conserved in eukaryotes and binds to microtubules in its C-terminal region. The EB1 domain is also conserved in eukaryotes from yeasts to human. It has been reported that EB1 function from yeast to human is regulated by phosphorylation, but its role is poorly understood and kinase of EB1 is not known [22].

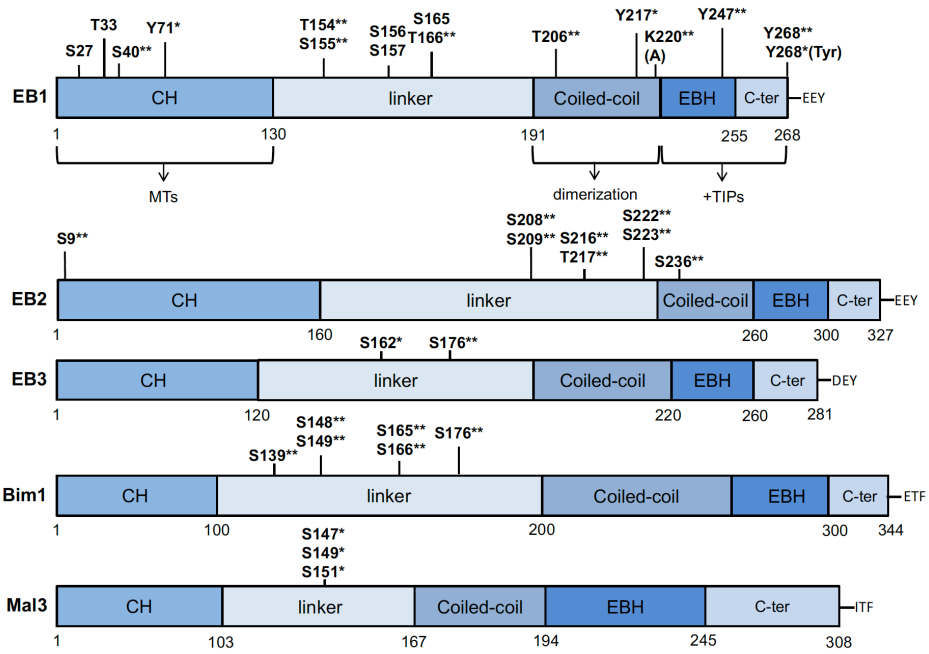

Fig. 1-4 Structural organization and post-translational modifications of EB orthologs.

Schematic diagram of functional domains and post-translational modifications among human EB1, EB2, EB3, and yeast Bim1 and Mal. *Two asterisks* indicate phosphorylation sites that are validated and their kinases are identified, and *one asterisk* in Mal3 indicates the validate phosphorylation sites but their kinases are not known. Note that K220(A) and Y268(Tyr) residues in EB1 are sites of acetylation and detyrosination, respectively. *CH,* calponin-homology; *EBH,* EB-homology (EB1);*C-ter,* Carboxy-terminal region. Amino-acid numbering is indicated below each EB polypeptide [cited from [22]]

Mal3 is an orthologue of the EB1 family protein in fission yeast. Beinhauer *et al.,* identified *mal3* as a gene that restored the phenotypes of the *mal3-1* mutant, which exhibited mini-chromosome loss and microtubule inhibitor sensitive phenotypes [23]. Mal3 regulates maintenance of cell polarity in interphase and chromosome segregation in mitosis. In interphase, Mal3 mainly localizes to the microtubule plus end and recruits the cell polarity regulatory proteins including Tea2, Tip1, Tea1/Tea4 complex [24,25][26]. The loss of functional Mal3 causes shorter microtubules and abnormal morphology such as bent and T-shape [23]. In mitosis, Mal3 binds to kinesin/Klp2, Blinkin/Spc7 and TOG/Dis1 but function of Mal3 is not completely understood [27–29].

Mal3 binds to the corner of tubulin dimer, through the CH domain of Mal3. The CH domain of Mal3 mutants have been analyzed for their microtubule binding activity by several groups. Mal3 (K63D) and Mal3 (Q89E) fail to bind to microtubules, while Mal3 (Q89A) and Mal3 (Q89R) bind excessively to microtubules, both *in vitro* and *in vivo* [30,31]. These mutants site is proximity site with four tubulin dimers. Q89R mutation of Mal3 causes hyper phosphorylation on the coiled-coil region of Mal3 [30].

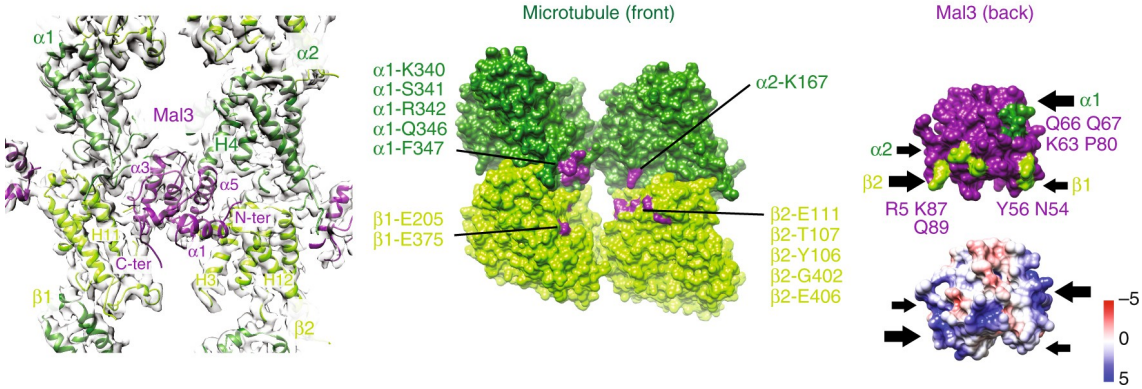

Fig. 1-5 Consequences of *S. pombe* microtubule architecture for Mal3 binding.

Left figure ; Mal3 contacts with α-tubulin1 and α-tubulin2 (dark green), β-tubulin1 and β-tubulin2 (light green). Middle figure ; The figure representing the tubulin surface which is considered to be contact with Mal3 surface. Mal3 contact site indicated purple. Right figure ; top, The figure representing the Mal3 surface which is considered to be contact with tubulin surface. Tubulin contact site indicated green and labeled; bottom, charge distribution of the Mal3 microtubule-binding surface. The black arrows indicate the four contact points of Mal3 with the microtubule. These contact sites is including microtubule binding activity mutants of Mal3. [cited from [32]]

The cAMP/PKA pathway

S. pombe predominantly utilizes glucose as carbon source. To survive in various environmental conditions, cells need to respond rapidly toward nutrient state, specifically, carbon source availability. Cyclic adenosine monophosphate (cAMP)-dependent protein kinase, also known as protein kinase A (PKA), is a serine/threonine kinase that is highly conserved from yeasts to mammals [33–36]. In fission yeast, the cAMP/PKA pathway consists of the G protein-coupled receptor Git3, a heterotrimeric G protein alpha subunit (Gpa2), a beta subunit (Git5), a gamma subunit (Git11), an adenylate cyclase (Cyr1), a protein kinase A regulatory subunit (Cgs1), and a protein kinase A catalytic subunit (Pka1). cAMP, generated by Cyr1 from adenosine triphosphate (ATP), binds with Cgs1, a regulatory subunit of PKA, to release Pka1, which then executes its catalytic activity [33,37–42]. This pathway is known to be involved in glucose repression, chronological aging, stress responses to KCl and $CaCl_2$, chromosome regulation, and regulation of transit from mitosis to meiosis [33,43–47]. However, much more unveiled biological roles of the cAMP/PKA pathway are expected.

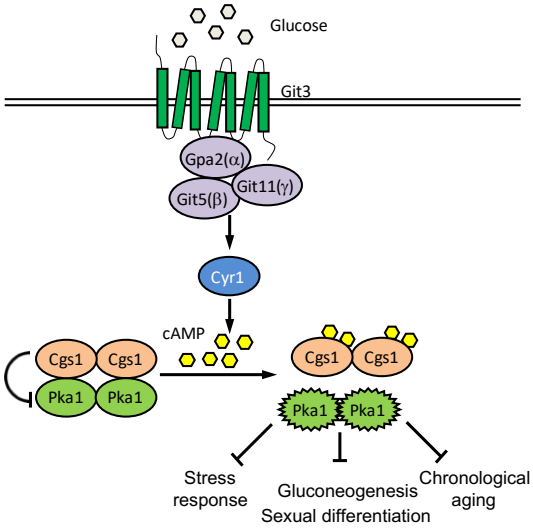

Fig. 1-6 The cAMP/PKA pathway in *S. pombe*

The cAMP/PKA pathway consists of the G protein-coupled receptor Git3, a heterotrimeric G protein alpha subunit (Gpa2), a beta subunit (Git5), a gamma subunit (Git11), an adenylate cyclase (Cyr1), a protein kinase A regulatory subunit (Cgs1), and a protein kinase A catalytic subunit (Pka1).

Chapter 2

Materials and methods

Yeast strains, media, and genetic methods

The *S. pombe* strains used in this study are listed in Table 2-1. Standard yeast culture media and genetic methods were used [48,49]. *S. pombe* cultures were grown in either YES medium (0.5% yeast extract, 3% glucose, 225 mg/L adenine, 225 mg/L uracil, 225 mg/L leucine, 225 mg/L histidine, and 225 mg/L lysine), YES glucose-limited medium (0.5% yeast extract, 0.1% glucose, 3% glycerol, 225 mg/L adenine, 225 mg/L uracil, 225 mg/L leucine, 225 mg/L histidine, and 225 mg/L lysine), or synthetic minimal medium (EMM) with appropriate auxotrophic supplements [48]. Mutant and transgenic strains were constructed by genetic crossing and selection with markers using standard yeast genetics techniques.

Table 2-1 *S. pombe* strains used in this study

Strain	Genotype	Source
PR109	*h⁻ leu1-32 ura4-D18*	P. Russell
YMP28	*h⁻ leu1-32 ura4-D18 cyr1::ura4*	[44]
YMP40	*h⁻ leu1-32 ura4-D18 cgs1::ura4*	[44]
YMP36	*h⁻ leu1-32 ura4-D18 pka1::ura4*	[44]
YMP58	*h⁻ leu1-32 ura4-D18 cyr1::LEU2 cgs1::ura4*	[44]
TTP1	*h⁻ leu1-32 ura4-D18 mal3::natMX6*	This study
TTP2	*h⁺ leu1-32 ura4-D18 mal3::natMX6*	[50]
TTP5	*h⁻ leu1-32 ura4-D18 cgs1::ura4 mal3::natMX6*	This study
TTP7	*h⁻ leu1-32 ura4-D18 pka1::ura4 mal3::natMX6*	This study
TTP3	*h⁻ leu1-32 ura4-D18 mal3-GFP(S65T)-natMX6*	[50]
TTP26	*h⁻ leu1-32 ura4-D18 cgs1::ura4 mal3-GFP(S65T)-natMX6*	This study
TTP20	*h⁻ leu1-32 ura4-D18 pka1::ura4 mal3-GFP(S65T)-natMX6*	This study
TTP4	*h⁻ leu1-32 ura4-D18 mal3-13Myc-natMX6*	This study
TTP24	*h⁻ leu1-32 ura4-D18 cgs1::ura4 mal3-13Myc-natMX6*	This study
TTP22	*h⁻ leu1-32 ura4-D18 pka1::ura4 mal3-13Myc-natMX6*	This study
MY273 (FY8144)	*h⁻ his2 ade6-M210 Ch16*	NBRP
TTP101	*h⁻ ade6-M210 leu1-32 ura4-D18 Ch16*	This study
TTP104	*h⁻ ade6-M210 leu1-32 ura4-D18 pka1::ura4 Ch16*	This study
TTP69	*h⁺ ade6-M210 leu1-32 ura4-D18 Ch16*	This study
TTP70	*h⁺ ade6-210 leu1-32 ura4-D18 mal3::kanMX6 Ch16*	This study
TTP103	*h⁺ leu1-32 ura4-D18 sad1-mRFP-hphMX6*	This study

TTP110	*h+ leu1-32 ura4-D18 pka1::ura4 sad1-mRFP-hphMX6*	This study
TTP113	*h+ leu1-32 ura4-D18 mal3::naMX6 sad1-mRFP-hphMX6*	This study
TTP76	*h- leu1-32 ura4-D18 kanMX6-nmt81-GFP-atb2 sad1-mRFP-natMX6*	This study
TTP171	*h+ leu1-32 ura4-D18 kanMX6-nmt81-GFP-atb2 sad1-mRFP-hphMX6 mal3::natMX6*	This study
TTP218	*h- leu1-32 ura4-D18 kanMX6-nmt81-GFP-atb2 sad1-mRFP-natMX6 pka1::ura4*	This study
JW952 (FY13663)	*h- ade6-M210 leu1-32 ura4-D18 tor1::ura4*	NBRP
TTP233	*h- leu1-32 ura4-D18 tor1::ura4*	This study
MBY1748	*h- leu1-32 ura4-D18 ssp2::ura4*	
MY2187 (FY10087)	*h- leu1 ura4 cut7-446*	NBRP
YMP324	*h- leu1-32 ura4-D18 cut7-446*	This study
YMP351	*h- leu1-32 ura4-D18 pka1::ura4 cut7-446*	This study
TTP157	*h- leu1-32 ura4-D18 cut7-446 kanMX6-nmt81-GFP-atb2 sad1-mRFP-natMX6*	This study
TTP277	*h- leu1-32 ura4-D18 pka1::ura4 cut7-446 kanMX6-nmt81-GFP-atb2 sad1-mRFP-natMX6*	This study
JW217 (FY13543)	*h90 ade6-M216 leu1-32 ura4-D18 tip1::ura4*	NBRP
JX527 (FY13477)	*h- ade6-M210 leu1-32 ura4-D18 ssm4::ura4*	NBRP
TTP223	*h- leu1-32 ura4-D18 tip1::ura4*	This study
TTP224	*h- leu1-32 ura4-D18 ssm4::ura4*	This study
PB871 (FY31472)	*h90 ade6? ura4? leu1-32 cut11-7 pkl1::kanMX6 klp2::LEU2 mad1(K24A K25A) GFP-atb2-ura4 mis6-2mCherry-bsd sfi1-CFP-natMX6*	NBRP
TTP254	*h- leu1-32 ura4-D18 klp2::LEU2*	This study

Plasmid construction and induction of expression under the nmt1 promoter

The oligonucleotide primers used for plasmid construction in this study are listed in Table 2-2. To construct pGBKT7-Mal3, the oligonucleotide primers Mal3-BF and MAL3-SSR were used to amplify a 927 bp fragment containing the complete *mal3* protein coding sequence from *S. pombe* cDNA. The amplified *mal3* gene fragment was digested with *Bam*HI and *Sal*I and ligated into the corresponding sites of pGBKT7 (Clontech) to generate the plasmid pGBKT7-Mal3. To construct pGBKT7-Mal3 (1–143), pGBKT7-Mal3 (1–197), pGBKT7-Mal3 (1–218), pGBKT7-Mal3 (1–241), and pGBKT7-Mal3 (135–308), the pGBKT7-Mal3 plasmid was used as the template DNA. The oligonucleotide primer set MAL3-BF and MAL3-143SSmR for pGBKT7- Mal3 (1–143), the primer set MAL3-BF and MAL3-197SSmR for pGBKT7- Mal3 (1–197), the primer set MAL3-BF and MAL3-218SSmR for pGBKT7- Mal3 (1–218), the primer set MAL3-BF and MAL3-241SSmR for pGBKT7- Mal3 (1–241), and the primer set MAL3-135BF and MAL3-SSR for pGBKT7-Mal3 (135–308) were used to construct the corresponding plasmids. To construct pGAD424-Mal3, pGAD424-Mal3 (1–143), pGAD424-Mal3 (1–197), pGAD424-Mal3 (1–218), pGAD424-Mal3 (1–241), and pGAD424-Mal3 (135–308), each of the pGBKT7-derived plasmids was digested with *Bam*HI and *Sal*I and ligated into the corresponding sites of pGAD424 (Clontech).

To construct pREP3X-Mal3, pREP3X-Mal3 (1–143), pREP3X-Mal3 (1–197), pREP3XMal3 (1–218), pREP3X-Mal3 (1–241), and pREP3X-Mal3 (135–308), each of the pGBKT7-derived plasmids was digested with *Bam*HI and *Sma*I and cloned into the corresponding sites of pREP3X [51]. To construct pREP3X-Mal3 (Q89E) and pREP3X-Mal3 (Q89R), pGBKT7-Mal3 plasmid was used as the template DNA. The oligonucleotide primer sets MAL3-BF/MAL3(Q89E)-R and MAL3(Q89E)-F/MAL3-SSR were used to construct pREP3X-Mal3(Q89E), and the primer sets MAL3-BF/MAL3(Q89R)-R and MAL3(Q89R)-F/MAL3-SSR were used to construct pREP3X-Mal3 (Q89R). To construct pREP3X-Mal3 (135-241), the oligonucleotide primers MAL3-135BF and MAL3-241SSmR were used to amplify a 340 bp fragment from pREP3X-Mal3. The amplified *mal3* (135-241) fragment was digested with *Bam*HI and *Sma*I and ligated into corresponding sites in pREP3X to generate the plasmid pREP3X-Mal3 (135-241).

Construction of pREP3X-Mal3 (1-241 Q89E) was performed according to the method described previously using pREP3X-Mal3 (1-241) as a template. To analyze whether the level of Mal3 expression affected phenotypes, pREP41X-mal3, containing the *nmt41* promoter rather than the *nmt1* promoter, was constructed using the restriction enzymes *Bam*HI and *Sma*I from pREP3X-Mal3 and pREP41X. Other plasmids used were described previously.

The plasmids pEGFP-N-human EB1 [52] and pGFP-NKB-mouse EB1 [53] were used as the template and the oligonucleotide primer sets HsMAPRE1-XF and HsMAPRE1-BR, and MmMAPRE1-XF and MmMAPRE1-BR were used to construct pREP3X-HsMAPRE1 (human EB1) and pREP3X-MmMAPRE1

(mouse EB1), respectively. The plasmids pET32-FHP-ATEB1a, pET32-FHP-ATEB1b, and pET32-FHP-ATEB1c[54] were used as the template and the oligonucleotide primer sets ATEB1a-SF and ATEB1a-BR, ATEB1b-SF and ATEB1b-BR, and ATEB1c-SF and ATEB1c-BR were used to construct pREP3X-AtEB1a (*Arabidopsis thaliana* EB1), pREP3X-AtEB1b (*A. thaliana* EB1b), and pREP3X-AtEB1c (*A. thaliana* EB1c), respectively. *Saccharomyces cerevisiae* genomic DNA was used as the template and the oligonucleotide primer set BIM1-SF and BIM1-BR was used to construct pREP3X-BIM1 (*S. cerevisiae* EB1).

To construct pGBKT7-Tip1, the oligonucleotide primers Tip1-BF and Tip1-SSR were used to amplify a 1,386 bp fragment containing the complete *tip1* protein coding sequence from *S. pombe* genomic DNA. The amplified *tip1* gene fragment was digested with *Bam*HI and *Sal*I and ligated into the corresponding sites of pGBKT7 to generate the plasmid pGBKT7-Tip1. To construct pGAD424-Tip1, the plasmid pGBKT7-Tip1 was digested with *Bam*HI and *Sal*I and ligated into the corresponding sites of pGAD424.

S. pombe genomic DNA from the Mal3-GFP strain (TTP3) was used as the template and the oligonucleotide primer set MAL3-BF and GFP-SR was used to construct pREP41X-Mal3-GFP. To construct pREP41X-Mal3(1–143)-GFP and pREP41X-Mal3(135–308)-GFP, the plasmids pREP41X-Mal3-GFP was used as the template and the oligonucleotide primer sets MAL3-BF, MAL3(1–143)GFP-F, MAL3(1–143)GFP-R, and GFP-SR for pREP41X-Mal3(1–143)-GFP, and MAL3-135BF and GFP-SR for pREP41X-Mal3(135–308)-GFP were used. The amplified fragments were digested with *Bam*HI and *Sma*I sites, and ligated into the appropriate sites of pREP41X.

Wild-type, *mal3*Δ, *pka1*Δ, *tor1*Δ, *ssp2*Δ *tip1*Δ*, and ssm4*Δ cells were transformed with the pREP3X-derived plasmids (*LEU*2 marker) and transformants were selected onto EMMU (EMM containing uracil but lacking leucine) plates containing 15 μM thiamine to repress gene expression from the *nmt1* promoter. To test the growth following *mal3* overexpression, transformants were grown on EMMU containing 15 μM thiamine for 2 days at 30°C, and were then transferred onto EMMU without thiamine, to induce *mal3* expression from the *nmt1* promoter, and incubated for 1 day at 30°C. Cells were then spotted on EMMU plates in the presence or absence of 15 μM thiamine and incubated for 3 to 5 days at 30°C.

When *mal3* expression was induced from the *nmt1* promoter, cells were first grown in EMM containing 15 μM thiamine to mid-log phase (~5 x 10^6 cells/mL) at 30˚C. The cells were then washed three times with water and resuspended in EMM lacking thiamine and incubated for an additional 24 h at 30˚C.

Table 2-2 Oligonucleotide primers used for making plasmids in this study.

Primer name	Sequence
MAL3-BF	5'-TATGGATCCTCATGTCTGAATCTCGGCAAGAG-3'
MAL3-SSR	5'-ACAGTCGACCCGGGTTAAAACGTGATATTCTCATC-3'
MAL3-135BF	5'-TATGGATCCTCATGACTGGCCCTTCTCGTCGCCGTC-3'
MAL3-143SSmR	5'- ACAGTCGACCCGGGTTAAACCTGACGGCGACGAGAAG-3'
MAL3-197SSmR	5'-ACAGTCGACCCGGGTTAACCAAACATCGTCTCATTAAC-3'
MAL3-218SSmR	5'-ACAGTCGACCCGGGTTAAGTTTGTACAAGTATTTCAAT-3'
MAL3-241SSmR	5'-ACAGTCGACCCGGGTTAAGTAGAATAAAGTATTGCTTG-3'
MAL3(Q89E)-F	5'-TTGTAAAATGGAAGATAATCT-3'
MAL3(Q89E)-R	5'-AGATTATCTTCCATTTTACAA-3'
MAL3(Q89R)-F	5'-TTGTAAAATGAGAGATAATCTG-3'
MAL3(Q89R)-R	5'-CAGATTATCTCTCATTTTACAA-3'
HsMAPRE1-XF	5'-TATCTCGAGATGGCAGTGAACGTATACTC-3'
HsMAPRE1-BR	5'-ACAGGATCCTTAATACTCTTCTTGCTCCTC-3'
MmMAPRE1-XF	5'-TATCTCGAGATGGCAGTGAATGTGTACTC-3'
MmMAPRE1-SmR	5'-ACACCCGGGTTAATACTCTTCTTGTTCCTC-3'
ATEB1a-SF	5'-TATGTCGACATGGCGACGAACATCGGAATG-3'
ATEB1a-BR	5'-ACAGGATCCTTAGGCTTGAGTCTTTTCTTC-3'
ATEB1b-SF	5'-TATGTCGACATGGCGACGAACATTGGGATG-3'
ATEB1b-BR	5'-ACAGGATCCTTAAGTTTGGGTCTCTGCAG-3'
ATEB1c-SF	5'-TATGTCGACATGGCTACGAACATTGGGATG-3'
ATEB1c-BR	5'-ACAGGATCCTCAGCAGGTCAAGAGAGGAG-3'
BIM1-SF	5'-TATGTCGACATGAGTGCGGGTATCGGAGAATC-3'
BIM1-BR	5'-ACAGGATCCTTAAAAAGTTTCCTCGTCGATG-3'
MAL3(1-143)GFP-F	5'-CTTCTCGTCGCCGTCAGGTTTCGTACGCTGCAGGTCGACG-3'
MAL3(1-143)GFP-R	5'-CGTCGACCTGCAGCGTACGAAACCTGACGGCGACGAGAAG-3'
GFP-SR	5'-ACACCCGGGAGATCTATATTACCCTGTTA-3'
TIP1-BF	5'-TATGGATCCAAATGTTTCCTCTTGGCAGTGTC-3'

TIP1-SSR	5'-ACAGTCGACCCGGGTTAAGCTTCGTCTGTGCTG-3'

Yeast two-hybrid system

The yeast Matchmaker Two-Hybrid System 3 (Clontech) was used to examine the *in vivo* self-interaction of the truncated Mal3 proteins. For the assays, the plasmids of two fusion constructs into pGBKT7 (a Gal4 DNA-binding domain vector for Gal4-BD fusion) and pGAD424 (a Gal4-activating domain vector for Gal4-AD fusion) were then co-introduced into AH109 yeast cells using the lithium acetate method. Transformed yeast cells were grown on the synthetic dextrose medium (SC) lacking leucine and tryptophan (SC-LW) plate, for 3 days at 30˚C. The specific protein-protein interaction was determined by the growth of yeast cells on SC medium lacking leucine, tryptophan, and histidine (SC-LWH).

Mini-chromosomal loss assay

This assay was performed as previously described [55]. Two independent Ade^+ isolates of the wild type, *pka1*Δ, and *mal3*Δ strains, were analyzed for the stability of the mini-chromosome16 (Ch16) containing the *ade6-M210* mutation, on adenine-limited EMMU plates, in the presence or absence of 7.5 μg/mL TBZ. The host *ade6-M210* cells are rendered Ade^+ by allelic complementation. Transformed cells were plated on adenine-limited EMMU plates in the presence or absence of 7.5 μg/mL TBZ and incubated at 30˚C for 3 to 5 days and then at 4˚C for 1 to 2 overnight periods to allow deepening of the red color of the Ade^- colonies. The frequency of chromosome loss was determined by counting the total colonies and the red colonies.

Fluorescence microscopy of GFP or mRFP fusion protein

S. pombe cells were grown in EMMU liquid medium containing 15 μM thiamine, washed three times with water, transferred to EMMU liquid medium lacking thiamine, and incubated for 24 h at 30°C. GFP-tagged Atb2 and mRFP-tagged Sad1 proteins in living cells were visualized and imaged using a BX51 microscope (Olympus) equipped with a DP74 digital camera (Olympus) or on a BZ-X700 microscope (Keyence).

Preparation of cell lysates and detection of Mal3 protein or 13Myc fusion protein by immunoblotting

S. pombe cell lysates were prepared as previously described [56]. Protein lysates were separated by SDS-PAGE, after which western blot analysis was performed using an ECL detection system (GE

Healthcare) according to the supplier's instructions. Rabbit polyclonal anti-Mal3 (diluted 1:1000) antibody was provided by Drs. M. Iimori (Kyushu University) and T. Matsumoto (Kyoto University). Mouse monoclonal anti-Myc (diluted 1:1000), and Rabbit polyclonal anti-PSTAIRE (Cdc2; diluted 1:1000) antibody was purchased from Santa Cruz Biotechnology. Horseradish peroxidase-conjugated anti-rabbit IgG antibody (Promega) was used as the secondary antibody.

Fluorescence-activated cell sorting (FACS) of DNA contents

Cells were cultured to mid-log phase in EMMU containing 15 μM thiamine at 30˚C, washed three times with water, resuspended in EMMU without thiamine, and cultured for 24 h at 30˚C. Cells were then fixed for 1 day on ice using 70% ethanol and washed with 50 mM sodium citrate. Fixed cells were suspended into 0.1 mL of 50 mM sodium citrate containing 1 mg/mL RNase A and incubated for 3 h at 37˚C. After RNA degradation, the suspended cells were stained with 2 μg/mL propidium iodide. Stained cells were analyzed using a FACSCalibur flow-cytometer (Becton-Dickinson).

Data and statistics

Experiments were performed in triplicate and the average values and standard deviation (SD) were calculated. Data from controls and cells overexpressing Mal3 were compared using a two-sample *t*-test. P-values <0.05 were considered statistically significant. All statistical analyses were performed using EZR version 3.61 (Saitama Medical Center, Jichi Medical University, Saitama, Japan) [57], which is a graphical user interface for R (The R Foundation for Statistical Computing, Vienna, Austria).

Reproducibility

Experiments were conducted at least twice to confirm the reproducibility of the results.

Chapter 3

Mal3 is a multi-copy suppressor of the sensitivity to microtubule-depolymerizing drugs and chromosome mis-segregation in a fission yeast *pka1* mutant

Introduction

Microtubules are the major cytoskeletal fibers in eukaryotic cells, which maintain the structure of cells and provide platforms for substance transport. Microtubules grow by the polymerization of the tubulin dimer, which consists of the α-tubulin and ß-tubulin, and shrink by depolymerization. In mitosis, microtubules dramatically change their structure and regulate chromosome segregation. Microtubule associated proteins (MAPs), such as XMAP215, EB1, CLIP170, and CLASP1, regulate microtubule function and stability [5,6]. Microtubule destabilizing drugs such as nocodazole, benomyl, thiabendazole (TBZ), and carbendazim (MBC), inhibit microtubule polymerization, especially that of ß-tubulin, resulting in shorter microtubules. These microtubule destabilizing drugs have benzimidazole as a basal structure and are used as anti-fungal and anti-helminthic drugs [58,59]. Because TBZ and MBC inhibit microtubules formation and cause chromosome mis-segregation, these drugs have been used to understand the mechanism of microtubule formation and chromosome segregation [60,61]. EB1 was first isolated as a protein that interacts with the C-terminus of adeno tumor polyposis coli, by screening in a yeast two-hybrid system [20]. EB1 is one of the MAPs that bind to microtubules, especially at the microtubules plus-end, and therefore, is known as a plus-end tracking protein (+TIP) [26], which also include EB1, CLIP-170, XMAP215, and CLASP1 [6]. The +TIP proteins play a role in the proper formation of microtubules, cell polarity, and cell elongation [6]. EB1 has the Calponin homology (CH) domain at the N-terminus, the coiled coil domain in the middle, and the end-binding (EB1) domain at the C-terminus [62]. The CH and the coiled-coil domains are responsible for the dimerization of EB1 [63]. The EB1 domain plays a role in the interaction with binding partners such as EB1, CLIP-170 and CLASP1 [5].

Mal3, in the fission yeast *S. pombe*, is a homolog of EB1, which is required for microtubule integrity and the maintenance of cell morphology [23]. The deletion of *mal3* gene results in shorter microtubules increases the loss of mini-chromosome during chromosome segregation, and exhibits the TBZ-sensitive phenotype [23]. Mal3 mutants have been analyzed for their activity on microtubule binding by several groups. Mal3 (K63D) and Mal3 (Q89E) fail to bind to microtubules, while Mal3 (Q89A) and Mal3 (Q89R) bind excessively to microtubules, both in vitro and in vivo [30,31]. Mal3 (Q89R) causes hyper phosphorylation on the coiled-coil region of Mal3 [30]. However, the kinase responsible for the phosphorylation of Mal3 has not been identified. The cyclic adenosine monophosphate (cAMP)-dependent protein kinase, also known as protein kinase A (PKA), is a serine/threonine kinase that is highly conserved among organisms ranging from yeasts to mammals [33–36]. cAMP, generated by the adenylate cyclase (Cyr1), from adenosine triphosphate (ATP), binds with Cgs1, a regulatory subunit of PKA, to release and activate Pka1 [37–39]. In *S. pombe*, this pathway is known to be involved in glucose repression, chronological aging, regulation of transit from mitosis to meiosis, and stress responses to KCl and $CaCl_2$

[33,43–47]. However, the biological roles of the cAMP/PKA pathway are not fully understood. In this study, the author and Yamaga found that *pka1Δ* showed the TBZ-sensitive and chromosome mis-segregated phenotypes. Yamaga screened multi-copy suppressors from a *S. pombe* cDNA library that suppress the TBZ-sensitive phenotype of the *pka1Δ* strains and isolated the *mal3* gene (unpublished results). Domain analysis revealed that the CH domain of Mal3 is sufficient for the multi-copy suppression of the TBZ-sensitive and chromosome mis-segregated phenotypes in the *pka1Δ* and *mal3Δ* strains. The author shows here the novel role of Pka1 in microtubule organization and proposed a novel function for the Mal3 CH domain.

Results

Multi-copy Mal3 suppresses the TBZ and MBC sensitive phenotype of *pka1*Δ strains.

To gain further the insight into the novel functions of Pka1 in *S. pombe*, the sensitivity of the wild type, *cgs1*Δ, and *pka1*Δ strains toward various drugs were tested. While the wild type and *cgs1*Δ strains grew on YES containing 0.1 μM Latrunculin A (LatA), 15 μg/mL thiabendazole (TBZ), 5 μg/mL carbendazim (MBC), or 1M KCl, the *pka1*Δ strain did not on 0.1 μM LatA or 1M KCl containing media as previously shown [39,41,44,64]. The author and Yamaga found the *pka1*Δ strain also exhibited growth retardation by 15 μg/mL TBZ and 5 μg/mL MBC (Fig. 3-1A), which are microtubule-destabilization drugs. The author next analyzed the role of Cyr1 and its dependency of Pka1 activity on the growth retardation phenotype by TBZ. The author found that the *cyr1*Δ strain exhibited the TBZ-sensitive phenotype at the concentration of 18 μg/mL TBZ, as similarly observed in the *pka1*Δ strain, and deletion of *cgs1* reversed its phenotype (Fig. 3-1B). Deletion of *cyr1* results in the inactivation of Pka1 and concomitant deletion of *cgs1* results in the constitutive activation of Pka1. These findings indicate that the TBZ-sensitive phenotype in the *cyr1*Δ strain is dependent on the Pka1 activity.

Because this phenotype of the *pka1*Δ strains was novel, the author first analyzed mitotic microtubule of the *pka1*Δ strain. Both the wild type and *pka1*Δ strains showed normal mitotic microtubules structure in the presence of TBZ similar to its absence (Fig. 3-1D). Because mitotic microtubules of the *pka1*Δ strain was indistinguishable with the wild type strain, Yamaga next conducted a screening for a multi-copy suppressor to identify the possible target of Pka1. The *pka1*Δ strain was transformed with pREP3X-*S. pombe* cDNA library, which is under the control of thiamine-repressible nmt1 promoter, and screened on EMMU containing 15 μg/mL TBZ. As a result, Yamaga obtained 15 candidates including Mal3, which is a microtubule plus-end EB1 family protein. Next, the author examined whether Mal3 is a specific multi-copy suppressor for the TBZ-sensitive phenotype of the *pka1*Δ strain (unpublished results). Toward this, the *pka1*Δ strain was transformed with pREP3X, pREP81-*pka1*, or pREP3X-*mal3* and the transformed cells

were spotted onto EMMU plates in the presence or absence of 15 μg/mL TBZ. Overexpression of Mal3 clearly rescued the TBZ-sensitive phenotype of the *pka1*Δ strains, although it did not rescue the growth on 1M KCl or 0.1 μM LatA (Fig. 3-1C). These results indicate that Mal3 is a specific multi-copy suppressor for TBZ sensitivity in the *pka1*Δ strain.

To exclude the possibility of Mal3 abnormality in the *pka1*Δ strains, the author analyzed the expression and localization of Mal3 in the Mal3-13Myc *pka1*Δ and Mal3-GFP *pka1*Δ strains. As a result, the expression of Mal3-13Myc was not affected in the MBC treated *pka1*Δ strains (Fig. 3-1E). Mal3-GFP was also normally localized at the microtubule in the *pka1*Δ strains after treatment with 20 μg/mL TBZ (Fig. 3-1F). These results indicate that the function of Mal3 was not depressed in the *pka1*Δ strains. Because the *mal3*Δ strain exhibited the TBZ-sensitive phenotype similar to the *pka1*Δ strains [23,29], the author analyzed the genetic interaction between Pka1 and Mal3 by growing the *cgs1*Δ *mal3*Δ and *pka1*Δ *mal3*Δ double mutants on YES containing TBZ. As shown in Fig. 3-1G, the wild type and *cgs1*Δ strains were not sensitive to TBZ, but the *cgs1*Δ *mal3*Δ double mutant as well as the *mal3*Δ strains exhibited sensitivity to 15 μg/mL TBZ. The TBZ sensitivity of the *pka1*Δ *mal3*Δ double mutant, however, was enhanced as it did not grow on a lower concentration of TBZ (10 μg/mL TBZ) compared with the *pka1*Δ or *mal3*Δ strains. The *cgs1*Δ strain also exhibited the TBZ-tolerance phenotype compared to the wild type strain (Fig. 3-1G). Furthermore, the author investigated whether the sensitivity of microtubule polymerization inhibitors of *mal3* deletion strains was suppressed by overexpression of *pka1*. As a result, the sensitivity of *mal3* deletion strains was not suppressed (Fig. 3-1H). The result, that the deletion of *pka1* enhances the TBZ sensitivity of the *mal3*Δ strain, suggests that Pka1 has other targets in addition to Mal3.

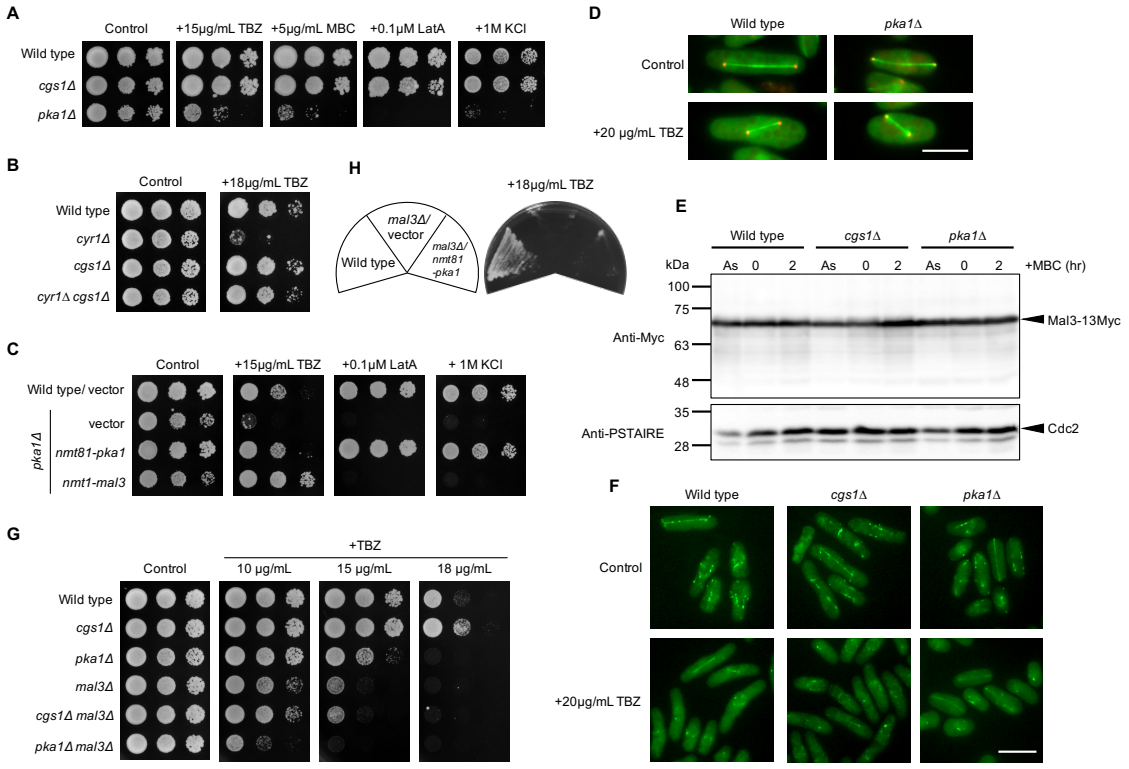

Fig. 3-1. Overexpression of Mal3 suppresses the TBZ-sensitive phenotype of the *pka1*Δ strains.

(A) Wild type (PR109), *cgs1*Δ (YMP40), and *pka1*Δ (YMP36) *S. pombe* strains were grown on YES, harvested, and resuspended in water at 107 cells/mL. The cell suspensions were serially diluted (1:10) and each dilution was spotted onto YES in the presence or absence of 15 μg/mL TBZ, 5 μg/mL MBC, 0.1 μM LatA, 1MKCl, and incubated for 5 days at 30˚C. (B) Wild type (PR109), *cyr1*Δ (YMP28), *cgs1*Δ (YMP40), and *cyr1*Δ *cgs1*Δ (YMP36) *S. pombe* strains were grown on YES, harvested, and resuspended in water at 10^7 cells/mL. Culture dilutions were prepared as described in Fig. 1A and spotted on YES in the presence or absence of 18 μg/mL TBZ. The plates were incubated for 3 or 5 days at 30˚C (YES for 3 days and YES+18μg/mL TBZ for 5 days). (C) The wild type (PR109) and *pka1*Δ (YMP36) strains harboring pREP3X (vector), pREP81-pka1, or pREP3X-mal3 were cultured for 1 day on EMMU (EMM with uracil) containing 15 μM thiamine at 30˚C to repress its expression of the *mal3* gene by the *nmt1* promoter. Cells were washed three times with water, transferred onto EMMU lacking thiamine and incubated for 24 h at 30˚C to induce *mal3* by the *nmt1* promoter. Culture dilutions were prepared as described above and spotted onto EMMU in the presence or absence of 15 μg/mL TBZ, 0.1 μM LatA, or 1M KCl. All plates were incubated for 5 days at 30˚C. (D) *GFP-atb2 sad1-mRFP* (TTP76) and *pka1Δ GFP-atb2 sad1-mRFP* (TTP218) strains were cultured in EMMLU (EMM+leucine+uracil) liquid medium to mid-log phase (~4 × 10^6cells/mL). Cells were cultured for 30 min in EMMLU liquid medium in the presence or absence of 20 μg/mL TBZ. Cells were observed by fluorescence microscopy. Green and red colors show GFP-Atb2 and Sad1-mRFP, respectively. Scale bar: 10 μm. (E) *mal3-13Myc* (TTP4), *cgs1Δ mal3-13Myc* (TTP24), and *pka1Δ mal3-13Myc* (TTP22) strains were cultured in YES liquid medium to mid-log phase (~4 × 10^6 cells/mL), and after addition of 10 mM HU, the cells were incubated for 4 h to arrest in the S phase. Cells were harvested by centrifugation and resuspended in YES with 50 μg/mL MBC, and further incubated for 2 h to prepare the cell lysates. To prepare asynchronous cells (As), the cells were cultured in YES liquid medium to mid-log phase (~4 × 10^6 cells/mL). Mal3-13Myc protein were detected by an anti-Myc antibody. Anti-PSTAIRE was used as an internal loading control. (F) *mal3-GFP* (TTP3), *cgs1Δ mal3-GFP* (TTP26), and *pka1Δ mal3-GFP*(TTP20) strains were cultured in YES liquid medium to mid-log phase (~4 × 10^6 cells/mL), and after addition of 10 mM HU, the cells were incubated for 4 h to arrest in the S phase. Cells were harvested by centrifugation and resuspended in YES with 20 μg/mL TBZ. Cells were observed by fluorescence microscopy at 2 h after incubation with TBZ. Scale bar: 10 μm. (G) Wild type (PR109), *cgs1*Δ (YMP40), *pka1*Δ (YMP36), *mal3*Δ (TTP1), *cgs1*Δ *mal3*Δ (TTP5), and *pka1*Δ *mal3*Δ (TTP7) *S. pombe* strains were grown on YES, harvested, and resuspended in water at 10^7 cells/mL. Culture dilutions were prepared as described in Fig. 3-1A and spotted on YES in the presence of absence of 10 μg/mL TBZ, 15 μg/mL TBZ, or 18 μg/mL TBZ. All plates were incubated for 5 days at 30˚C. (H) Wild type (PR109) and *mal3*Δ (TTP1) strains harboring pREP3X (vector), pREP81-pka1 were cultured as described in Fig. 3-1C. Cells were streaked on EMMU in the presence of 18 μg/mL TBZ. All plates were incubated for 4 days at 30˚C

Overexpression of the CH domain of Mal3 suppresses the TBZ-sensitive phenotype of the *pka1*Δ strain.

Mal3 has three domains namely, the Calponin homology (CH) domain at the N-terminus (3–103), a coiled-coil domain at the middle region (167–194), and an end binding (EB1) domain at the C-terminus (197–241) [30]. To identify which domain is important for the suppression of the TBZ sensitivity of the *pka1*Δ strains, the author constructed plasmids containing specific parts of Mal3 as shown in Fig. 3-2A. The author first analyzed the interaction of the Mal3 fragments by a yeast two-hybrid system. Mal3 (1–197), Mal3 (1–218), Mal3 (1–241), and Mal3 (135–308) interacted each other as well as with the full-length Mal3 (1–308) (Fig. 3-2B). However, Mal3 (1–143) did not interact with itself as in Fig. 3-2B and also as previously described [65].

Next, the author analyzed the suppression of the TBZ sensitivity of the *pka1*Δ strains by the individual domains. As shown in Fig. 3-2C, the overexpression of Mal3 (1–143) and Mal3 (1–197) rescued the TBZ-sensitive phenotype of the *pka1*Δ strains, while Mal3 (1–218) showed no effect. Mal3 (135–308) exhibited a growth defect in the *pka1*Δ strains at 12 μg/mL TBZ, and Mal3 (1–241) exhibited growth inhibition even in the absence of TBZ (Fig. 3-2C). Overexpression of the Mal3 CH domain is sufficient for the suppression of the TBZ sensitivity of the *pka1*Δ strains and the coiled-coil domain has a negative effect on growth (Fig. 3-2C). The author then analyzed the localization of Mal3 (full-length, 1–308) and Mal3 (1–143) by GFP fusion expressed under the *nmt41* promoter in the *pka1*Δ sad1-mRFP strain, to visualize the end points of the microtubules. As shown in Fig. 3-2D, the full-length of Mal3-GFP clearly localized to the microtubules in interphase and mitosis. The author did not observe any localization of Mal3 (1–143)-GFP in interphase, but detected localization on microtubules during prophase to anaphase in mitosis (Fig. 3-2D, arrowheads). These findings indicate that the microtubular localization of the CH domain of Mal3 is important, but its self-interaction is not required for the suppression of the TBZ sensitivity of the *pka1*Δ strains.

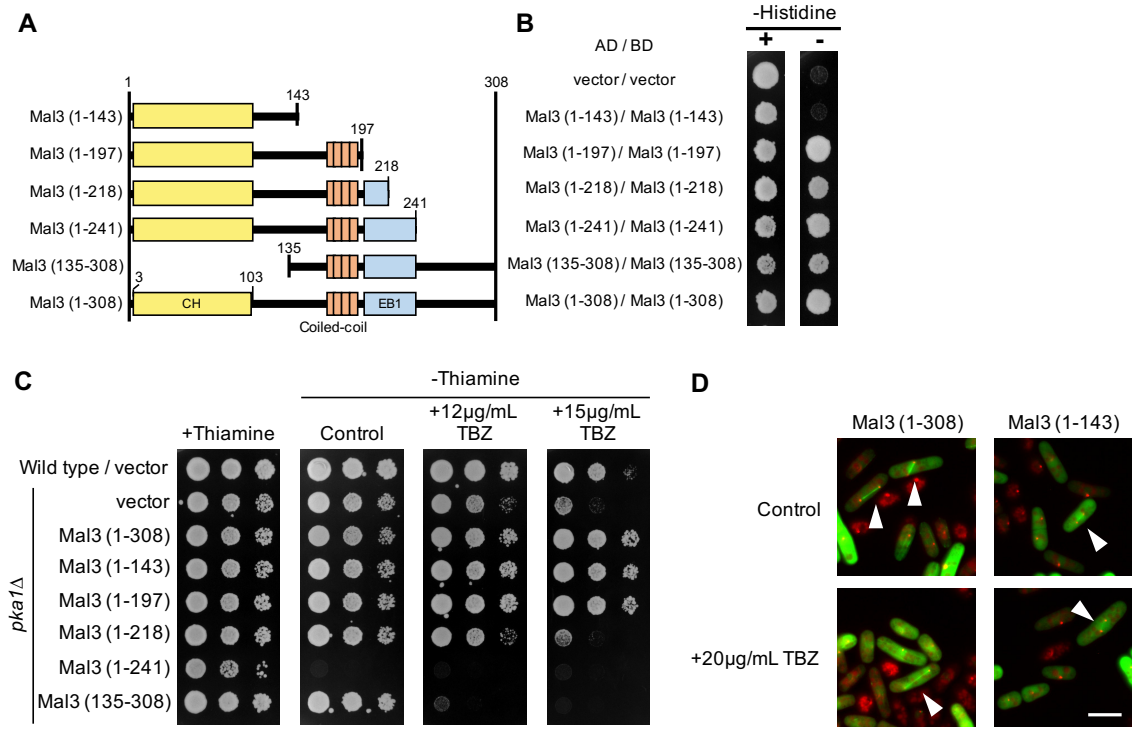

Fig. 3-2. Interaction of individual domains of Mal3 and the suppression of the TBZ-sensitive phenotype in the *pka1*Δ strains by the CH domain.

(A) The truncated Mal3 fragments used in this study. Mal3 has three domains; the CH domain (yellow), coiled-coil region (orange), and EB1 domain (blue). (B) *S. cerevisiae* AH109 strain was co-transformed with pGBKT7-derived plasmid and pGAD424-derived plasmid and selected on SC lacking leucine and tryptophan (SC-LW). Transformed cells were grown on SC-LW, harvested, and resuspended in water at 10^7 cells/mL. The cell suspensions were adjusted to 0.4 at OD600, spotted onto SC-LW in the presence or absence of histidine (SC-LW or SC-LWH), and incubated for 4 days at 30˚C. (C) Wild type (PR109) and *pka1*Δ (YMP36) strains harboring pREP3X (vector), pREP3X-mal3 (1–308: full-length), pREP3X-mal3 (1–143), pREP3X-mal3 (1–197), pREP3X-mal3 (1–218), pREP3X-mal3 (1–241), or pREP3X-mal3 (135–308) were cultured as described in Fig. 3-1C. Culture dilutions were prepared as described in Fig. 3-1A and spotted onto EMMU in the presence or absence of 12 μg/mL TBZ or 15 μg/mL TBZ. (D) *pka1*Δ Sad1-mRFP (TTP110) strains harboring pREP41-Mal3 (1–308)-GFP or pREP41-Mal3(1–143)-GFP was grown in EMMU containing 15 μM thiamine for 1 day at 30˚C. Cells were washed three times by water, transferred into EMMU without thiamine, and incubated for 24 h at 30˚C. Mal3-GFP (green color) and Sad1-mRFP (red color) were observed by fluorescent microscopy; Sad1 localizes to spindle pole body which is similar to centrosome in mammals. Sad1-mRFP was used to visualize the end of microtubules. Arrowheads indicate mitotic microtubules. Scale bar: 10 μm.

Microtubule binding ability of Mal3 is required for suppression and EB1 proteins from other eukaryotes suppress TBZ sensitivity in *pka1*Δ strains.

It has been previously reported that the Mal3 (Q89R) mutant strongly binds to the microtubules, and the Mal3 (Q89E) mutant does not [30,31]. We used the Mal3 mutants (Q89R and Q89E) to identify whether microtubule binding of Mal3 is required for the suppression TBZ sensitivity of the *pka1*Δ strains on EMM. As shown in Fig. 3-3A and Table 3-1, overexpression of the full-length Mal3 (Q89R) mutant caused growth inhibition in the *pka1*Δ strains in the absence of thiamine (control panel) and the full-length Mal3 (Q89E) weakly rescued the growth of the *pka1*Δ strains on 15 μg/mL TBZ. To further clarify the suppression by

the Mal3 mutants, the author next constructed the plasmids expressing the mutants of the CH domain: pREP3X-Mal3 (1–143 Q89E) and pREP3X-Mal3 (1–143 Q89R). Mal3 (1–143 Q89R) resulted in the rescue of the *pka1*Δ strains on EMM in the presence of 15 μg/mL TBZ or 5 μg/mL MBC, while Mal3 (1–143 Q89E) showed no effect on the *pka1*Δ strains on the same media (Fig. 3-3A and Table 3-1). These results indicate that the microtubule binding of Mal3 CH domain is important for the suppression of sensitivity to the microtubule-destabilizing drugs, in the *pka1*Δ strains.

Mal3 localizes to the microtubule plus end as a plus-end tracking protein (+TIP), thereby controlling cell morphology and microtubule dynamics in fission yeast. Therefore, the author next examined whether the other +TIP proteins such as Tip1 (CLIP-170), Tea1 (cell end marker), and Tea2 (kinesin), exhibit the suppression of the TBZ-sensitive phenotype of the *pka1*Δ strains. As a result, the overexpression of Tip1, Tea1, or Tea2 did not rescue the growth defect of the *pka1*Δ strains on EMM containing 15 μg/mL TBZ, although the overexpression of Tea2 caused growth defect under normal condition (Fig. 3-3C and Table 3-1). The author also examined the effect of the other microtubule binding proteins Alp7 (TACC protein) and Alp14 (TOG/XMAP215). As a result, Alp7 or Alp14 did not rescue the TBZ-sensitive phenotype of the *pka1*Δ strain (Fig. 3-3C and Table 3-1). These results indicate that the CH domain of Mal3 has a specific role in the suppression of sensitivity to the microtubule-destabilizing drugs of the *pka1*Δ strains.

Next, the author addressed whether the suppressive effect of Mal3 is conserved in higher eukaryotic EB1. To address this, the author examined the effect of human EB1 (HsEB1), mouse EB1 (MmEB1), A. *thaliana* EB1 (AtEB1a, AtEB1b, and AtEB1c), and S. *cerevisiae* Bim1p (ScEB1). As shown in Fig. 3B and Table 2, the overexpression of HsEB1, MmEB1, AtEB1a, and ScEB1 rescued the TBZ-sensitive or MBC-sensitive phenotype of the *pka1*Δ strains. However, the overexpression of AtEB1b and AtEB1c showed no effects on the growth of the *pka1*Δ strains on EMM with 15 μg/mL TBZ or 5 μg/mL MBC (Fig. 3-3B and Table 3-1). Therefore, the most of higher eukaryotic Mal3 orthologs as well as the budding yeast Mal3 have conserved function in regard to the suppression of TBZ-sensitive phenotype of the *pka1*Δ strains.

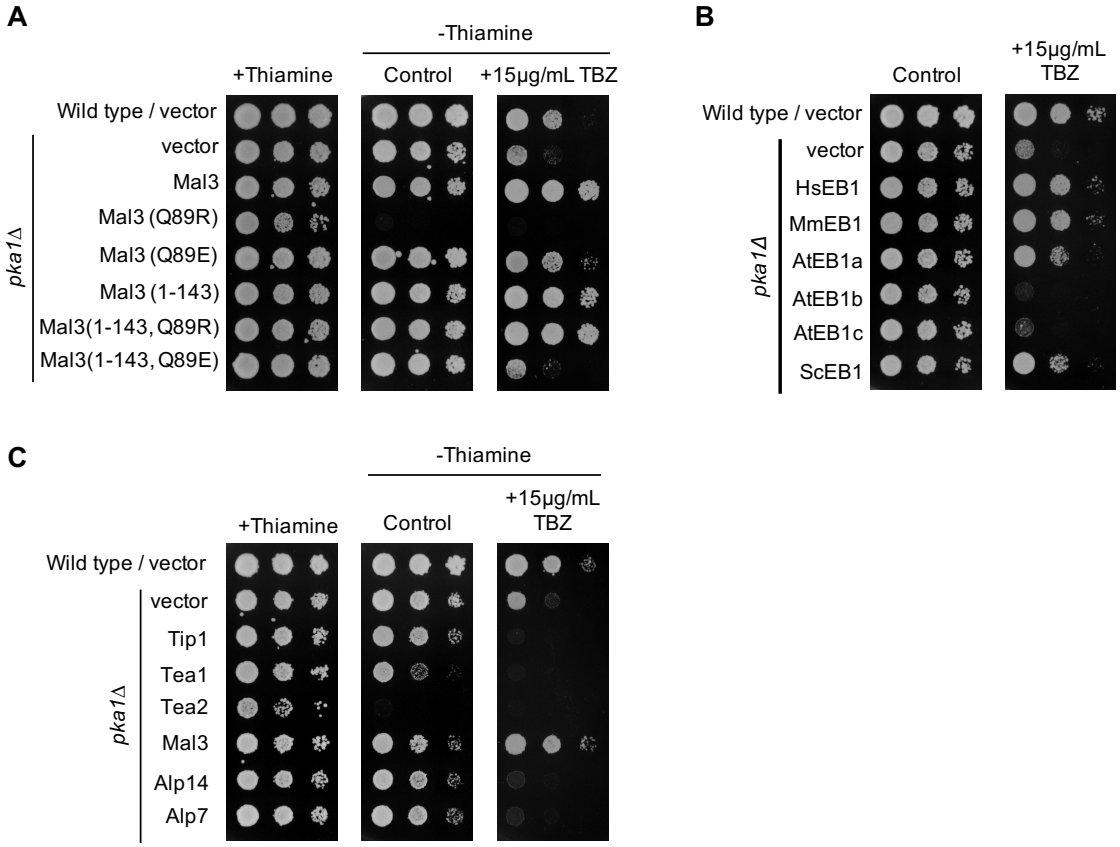

Fig. 3-3. Microtubule binding of Mal3 is responsible for the suppression of the TBZ-sensitive phenotype in the *pka1*Δ strains.

(A) Wild type (PR109) and *pka1*Δ (YMP36) strains harboring pREP3X (vector), pREP3X-mal3 (Q89R), pREP3X-mal3 (Q89E), pREP3X-mal3 (1–143), pREP3X-mal3 (1–143 Q89R), or pREP3X-mal3 (1–143 Q89E) were cultured as described in Fig. 3-1C. Culture dilutions were prepared as described in Fig. 3-1A and spotted on EMMU in the presence or absence of 15 μg/mL TBZ. All plates were incubated for 5 days at 30˚C. (B) Wild type (PR109) and *pka1*Δ (YMP36) strains harboring pREP3X (vector), pREP3X-HsMAPRE1 (HsEB1), pREP3X-MmMAPRE1 (MmEB1), pREP3X-AtEB1a (AtEB1a), pREP3X-AtEB1b (AtEB1b), pREP3X-AtEB1c (AtEB1c), or pREP3X-BIM1 (ScEB1) were cultured as described in Fig. 3-1C. Culture dilutions were prepared as described in Fig. 3-1A and spotted on EMMU in the presence or absence of 15 μg/mL TBZ. All plates were incubated for 5 days at 30˚C. (C) Wild type (PR109) and pka1Δ (YMP36) strains harboring pREP3X (vector), pREP3X-tip1, pREP3X-tea1, pREP3X-tea2, pREP3X-mal3, pREP41X-alp14, or pREP41X-alp7 were cultured as described in Fig. 3-1C. Culture dilutions were prepared as described in Fig. 3-1A and spotted on EMMU in the presence or absence of 18 μg/mL TBZ. All plates were incubated for 5 days at 30˚C.

Table 3-1 Growth profile of *pka1*Δ strains by overexpression of various Mal3 domains or orthologs

The TBZ sensitivity and the MBC sensitivity were analyzed by spotting assay and streak assay, respectively. N.T.: not tested.

Plasmid	No drug	+15 μg/mL TBZ	+5 μg/mL MBC	+10 μg/mL MBC
vector	+	-	-	-
Mal3 (1-308)	+	+	+	+
Mal3 (1-143)	+	+	+	-
Mal3 (1-197)	+	+	+	-
Mal3 (1-218)	+	-	-	-
Mal3 (1-241)	-	-	-	-
Mal3 (135-308)	+	-	-	-
Mal3 (Q89E)	+	+	+	-
Mal3 (Q89R)	-	-	-	-
Mal3 (1-143 Q89E)	+	-	-	-
Mal3 (1-143 Q89R)	+	+	+	-
HsEB1	+	+	+	-
MmEB1	+	+	+	-
AtEB1a	+	+	+	-
AtEB1b	+	-	-	-
AtEB1c	+	-	-	-
ScEB1	+	+	+	-
Tip1	+	-	N. T.	N. T.
Tea1	+	-	N. T.	N. T.
Tea2	-	-	N. T.	N. T.
Alp7	+	-	N. T.	N. T.
Alp14	+	-	N. T.	N. T.

Overexpression of Mal3 (1-143) suppresses chromosome mis-segregation induced by TBZ in the *pka1Δ* strain.

The observation that the Mal3 (1–143) rescues the TBZ-sensitive phenotype of the *pka1*Δ strains, and localizes to mitotic microtubules, led us to hypothesize that Mal3 (1–143) may suppress the chromosome mis-segregation of the *pka1*Δ strains. To address this, the author analyzed the chromosome segregation by the mini-chromosome loss assay. Because mini-chromosome Ch16 has the *ade6* gene and in the strains that have the *ade6-M210* mutation, the colonies show white color when the strains normally segregate the mini-chromosome, whereas the colonies show red color when the strains mis-segregated the mini-chromosome, on a plate containing low concentration of adenine [55]. Wild type strain harboring the vector exhibited white color colonies in the presence of 7.5 μg/mL TBZ, whereas the *pka1*Δ strain harboring the vector yielded approximately 0.5% red colonies in the absence of TBZ and approximately 2% red colonies in the presence of 7.5 μg/mL TBZ (Fig. 3-4A). Overexpression of the Mal3 (full-length), Mal3 (1–143), or Mal3 (1–197) rescued the mini-chromosome loss of the *pka1*Δ strain in the presence of TBZ (Fig. 3-4A). Next, the author analyzed the chromosome mis-segregation by DAPI staining using fluorescence microscopy. The wild type strain showed approximately 10% chromosome mis-segregation in the presence of 10 μg/mL TBZ, whereas the *pka1*Δ strains exhibited a high frequency (approximately 40%) of abnormal mitosis including the cut phenotype in which cells are separated by the septum before nuclear division and mis-segregated nucleus (Fig. 3-4B and 3-4C, and Table 3-2). Mal3 (full-length; 1–308), Mal3 (1–143), and Mal3 (1–197) overexpressing cells rescued the abnormal mitosis phenotype in the *pka1*Δ strains in the presence of 10 μg/mL TBZ (Fig. 3-4C and Table 3-2), indicating that the CH domain of Mal3 rescued the abnormal chromosome segregation in the *pka1*Δ strains.

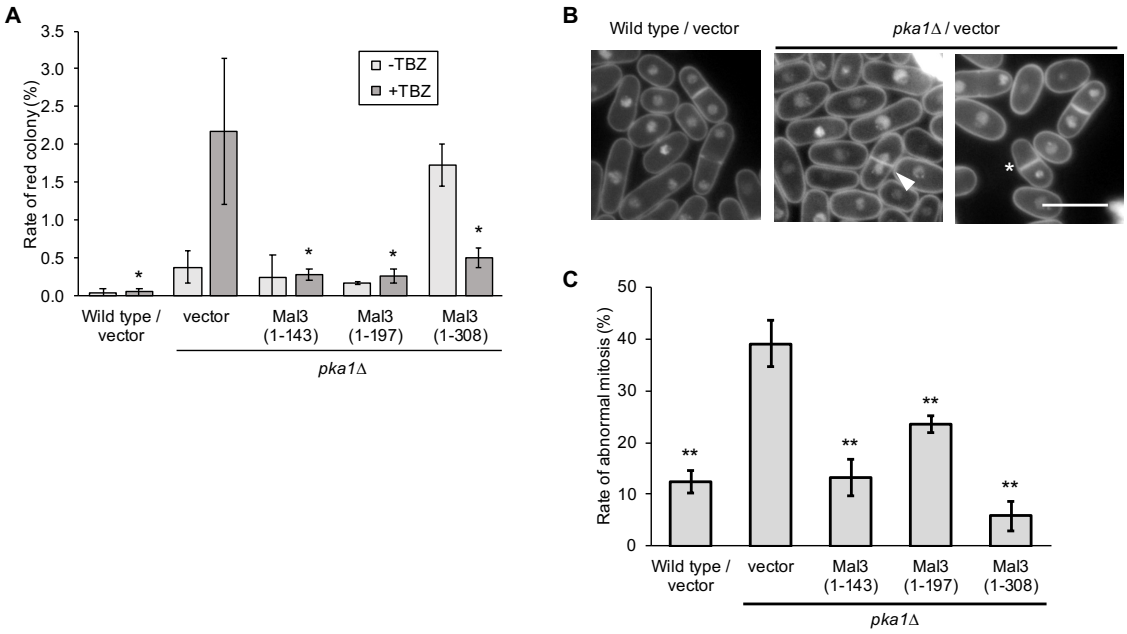

Fig. 3-4. Overexpression of Mal3 (1–143) suppresses chromosomal mis-segregation in the *pka1*Δ strains caused by the microtubule-destabilizing drugs.

(A) The wild type (TTP101) and *pka1*Δ (TTP104) strains harboring mini-chromosome Ch16 were transformed with pREP3X (vector), pREP3X-mal3 (1–143), pREP3X-mal3 (1–197), or pREP3X-mal3 (1–308; full-length). Cells were cultured as described in Fig. 3-1C. Cultured cells were platted on EMMU containing 10 μg/mL adenine in the presence or absence of 7.5 μg/mL TBZ. Plates were incubated for 7 days at 30˚C. Red colonies and sector colonies were counted. Experiments were performed three times: averages with S.D. are shown. Asterisks (*) indicate P-value < 0.05 for comparison with the *pka1*Δ strain harboring pREP3X (vector). (B) Wild type (PR109) and *pka1*Δ (YMP36) strains were cultured in YES. Cells were incubated with 10 μg/mL TBZ for 24 h at 18˚C. Cells were stained with DAPI and observed by fluorescent microscopy. Arrowhead and asterisk show the cut phenotype and mis-segregation, respectively. Scale bar: 10 μm. (C) Abnormal mitosis including the cut phenotype, in which cytokinesis takes place over the unseparated chromosomes and mis-segregation was determined by DAPI staining. About 50 cells were analyzed in individual strains and experiments were performed three times; averages with S.D. are shown. Double asterisks (**) indicate P-value < 0.01 for comparison with the *pka1*Δ strain harboring pREP3X (vector).

Table 3-2 The ratio of abnormal mitosis in the presence of 10 μg/mL TBZ

Strain	Plasmid	Mis-segregation (%)	Cut phenotype (%)	Total (%)
Wild type	vector	8.5 +/- 0.04	3.9 +/- 0.02	12.4 +/- 2.3
*pka1*Δ	vector	29.6 +/- 0.06	9.5 +/- 0.04	39.1 +/- 4.5
	Mal3 (1-143)	8.8 +/- 0.03	4.5 +/- 0.03	13.3 +/- 3.5
	Mal3 (1-197)	18.8 +/- 0.01	4.7 +/- 0.01	23.5 +/- 1.6
	Mal3 (1-308)	4.9 +/- 0.02	0.8 +/- 0.01	5.7 +/- 2.8

Overexpression of the Mal3 CH domain suppresses growth defect and chromosome mis-segregation in the presence of TBZ in *mal3*Δ strains.

It has been previously reported that *mal3*Δ results in the TBZ-sensitive phenotype and chromosome mis-segregation [23]. The author next analyzed whether the deletion of the CH domain causes the TBZ-sensitive phenotype in the *mal3*Δ strains. Toward this, the author used the plasmids expressing the fragmented and mutated Mal3. The overexpression of Mal3 (1–143), Mal3 (1–197), Mal3 (1–218), and Mal3 (1–308 full-length) rescued the growth of the *mal3*Δ strains on EMM in the presence of 15 μg/mL TBZ, whereas the overexpression of Mal3 (135–308) exhibited growth retardation on 12 μg/mL TBZ (Fig. 3-5A and Table 3-3). The overexpression of Mal3 (1–241) exhibited growth inhibition even in the absence of TBZ as observed in the *pka1*Δ strain (Fig. 3-5A and Table 3-3). Full-length Mal3 (Q89E) and Mal3 (Q89R) exhibited growth suppression on EMM containing TBZ and growth inhibition on EMM in the *mal3*Δ strain, respectively. Because these results might be due to the effect of the EB1 domain, the author next analyzed using the fragmented mutants of Mal3: Mal3 (1–143 Q89R) and Mal3 (1–143 Q89E). Overexpression of Mal3 (1–143 Q89R), which is an enhanced microtubule binding mutant, rescued the growth defect of the *mal3*Δ strains, similar to that observed in the *pka1*Δ strains, on EMM containing 15 μg/mL TBZ (Fig. 3-5A and Table 3-3) or 10 μg/mL MBC (Table 3-3). The mutant defective in microtubule binding, Mal3 (1–143 Q89E), did not restore the sensitivity to 15 μg/mL TBZ (Fig. 3-5A and Table 3-3) or 5 μg/mL MBC in the *mal3*Δ strains, similar to that observed in the *pka1*Δ strains (Table 3-3), indicating that the microtubule binding of Mal3 CH domain is required for the growth in the presence of microtubule-destabilizing drug.

Next, the author analyzed whether the CH domain is functional for proper chromosome segregation in the *mal3*Δ strains, by the mini-chromosome loss assay. As results, the overexpression of the Mal3 CH domain (1–143) or the Mal3 full-length (1–308) rescued the mini-chromosome loss in the *mal3*Δ strains, similar to that observed in the *pka1*Δ strains (Fig. 3-5B). These results indicate that the CH domain of Mal3 plays a role of maintenance in the normal segregation of chromosome.

Next, the author analyzed the suppression upon overexpression of other eukaryotic EB1s in the *mal3*Δ strains. Overexpression of *S. cerevisiae* Bim1p (ScEB1), human EB1 (HsEB1), mouse EB1 (MmEB1), and *A. thaliana* EB1a (AtEB1a) rescued the growth defect in the *mal3*Δ strains in the presence of 12 μg/mL TBZ but *A. thaliana* EB1b (AtEB1b) and EB1c (AtEB1c) failed to do so, as observed in the *pka1*Δ strains (Fig. 3-5C). These results indicate that the EB1 from yeasts to higher eukaryotes have conserved role in the restoration of growth defect in the presence of microtubule-destabilizing drugs.

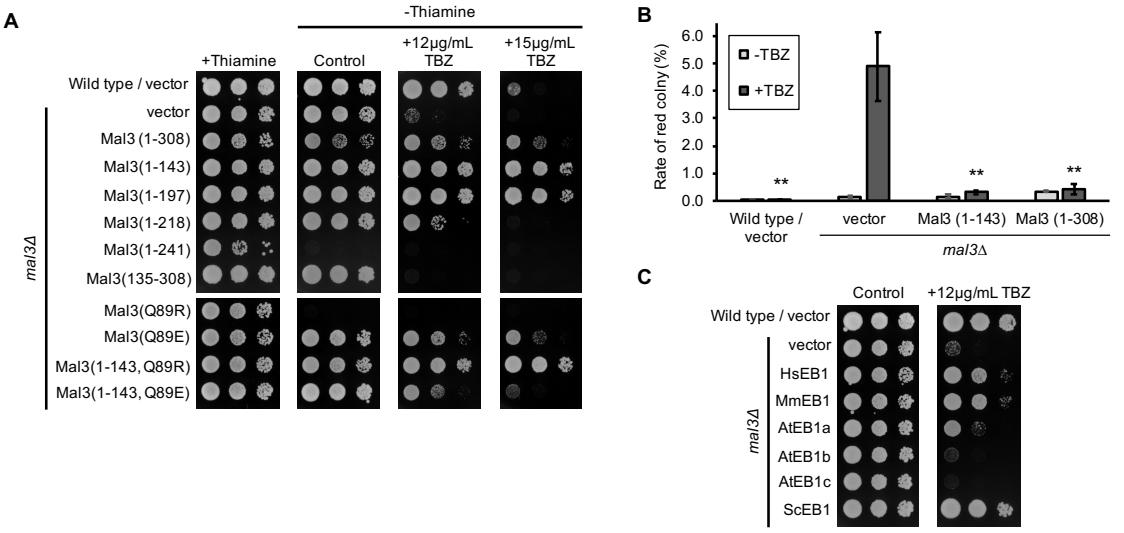

Fig. 3-5. Overexpression of Mal3 (1–143) suppresses the growth defect and chromosome mis-segregation caused by TBZ in the *mal3*Δ strains.

(A) Wild type (PR109) and *mal3*Δ (TTP1) strains harboring pREP3X (vector), pREP3X-mal3 (1–143), pREP3X-mal3 (1–308; full-length), pREP3X-mal3 (1–197), pREP3X-mal3 (1–218), pREP3X-mal3 (1–241), pREP3X-mal3 (135–308), pREP3X-mal3 (Q89R), pREP3X-mal3 (Q89E), pREP3X-mal3 (1–143 Q89R), or pREP3X-mal3 (1–143 Q89E) were cultured as described in Fig. 3-1C. Culture dilutions were prepared as described in Fig. 3-1A and spotted on EMMU in the presence or absence of 12 μg/mL TBZ or 15 μg/mL TBZ. All plates were incubated for 5 days at 30˚C. (B) Wild type (TTP69) and *mal3*Δ (TTP70) strains harboring the mini-chromosome Ch16 were transformed with pREP41X (vector), pREP41X-mal3 (1–143), or pREP41X-mal3 (1–308; full-length). Cells were cultured as described in Fig. 3-1C. Cultured cells were platted on EMMU containing 10 μg/mL adenine in the presence or absence of 7.5 μg/mL TBZ. Plates were incubated for 7 days at 30˚C. Red colonies and sector colonies were counted. Experiments were performed three times; averages with S.D. are shown. Double asterisks (**) indicate P-value < 0.01 for comparison with the *mal3*Δ strain harboring pREP3X (vector). (C) Wild type (PR109) and *mal3*Δ (TTP1) strains harboring pREP3X (vector), pREP3X-mal3, pREP3X-HsMAPRE1 (HsEB1), pREP3X-MmMAPRE1 (MmEB1), pREP3X-AtEB1a (AtEB1a), pREP3X-AtEB1b (AtEB1b), pREP3X-AtEB1c (AtEB1c), or pREP3X-BIM1 (ScEB1) were cultured as described in Fig. 3-1C. Culture dilutions were prepared as described in Fig. 3-1A and spotted on EMMU in the presence or absence of 12 μg/mL TBZ. All plates were incubated for 5 days at 30˚C.

Table 3-3 Growth profile of *mal3*Δ strains by overexpression of various Mal3 domains or orthologs

The TBZ sensitivity and the MBC sensitivity were analyzed by spotting assay and streak assay, respectively.

Plasmid	No drug	+15 μg/mL TBZ	+5 μg/mL MBC	+10 μg/mL MBC
vector	+	-	-	-
Mal3 (1-308)	+	+	+	+
Mal3 (1-143)	+	+	+	+
Mal3 (1-197)	+	+	+	+
Mal3 (1-218)	+	+	+	-
Mal3 (1-241)	-	-	-	-
Mal3 (135-308)	+	-	-	-
Mal3 (Q89E)	+	+	+	-
Mal3 (Q89R)	-	-	-	-
Mal3 (1-143 Q89E)	+	-	-	-
Mal3 (1-143 Q89R)	+	+	+	+
HsEB1	+	+	+	-
MmEB1	+	+	+	-
AtEB1a	+	+	+	-
AtEB1b	+	-	-	-
AtEB1c	+	-	-	-
ScEB1	+	+	+	-

Overexpression of the Mal3 CH domain give rise to the TBZ-tolerance in the wild type strain

As the author observed that overexpression of Mal3 (1–143) rescued the TBZ-sensitive phenotypes of *pka1*Δ and *mal3*Δ strains, the author analyzed the effect of Mal3 (1–143)-overexpression in wild type by looking at its phenotype. The wild type strain was transformed with pREP3x, pREP3x-mal3 (1–308; full-length), pREP3X-mal3 (1–143), or pREP3X-mal3 (135–308). Transformants were selected on EMMU in the presence of 15μMthiamine. To test the TBZ- sensitivity, transformants were cultured on EMMU in the absence of thiamine, transferred on EMMU in the presence or absence of TBZ, and incubated at 30 ˚C. As a result, overexpression of Mal3 (1–308) or Mal3 (1–143) did not alter their growth even with the presence of a high concentration of TBZ (60 μg/mL), although Mal3 (135–308)-overexpression caused inhibition of cell growth (Fig. 3-6A). This result suggests that the *pka1*Δ and *mal3*Δ strains were rescued by the TBZ-tolerance of the Mal3 CH domain (1–143).

Finally, the author tested the possibility that the Mal3 CH domain would affect the CLIP170 ortholog, Tip1. To do this, the author analyzed the interaction between the Mal3 CH domain and Tip1 by the yeast two-hybrid system. As a result, Mal3 (1–143) did not interact with Tip1 although Mal3 (1–308: full-length) interacted with Tip1 (Fig. 3-6B). This result suggests that the suppression of the Mal3 CH domain was not mediated by Tip1.

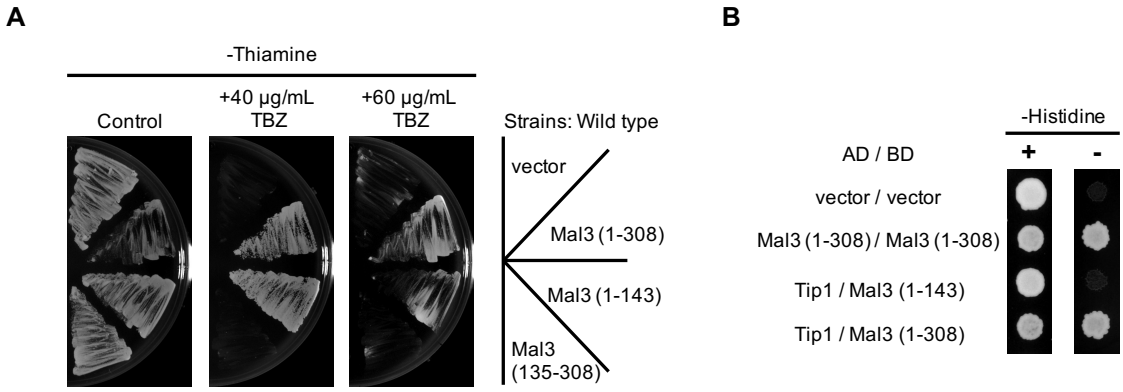

Fig. 3-6. Overexpression of Mal3 (1–143) exhibits the TBZ-tolerance in the wild type strain.
(A) Wild type (PR109) strains harboring pREP3X (vector), pREP3X-mal3 (1–308; full-length), pREP3X-mal3 (1–143), or pREP3X-mal3 (135–308) were cultured as described in Fig. 3-1C. Cells were streaked on EMMU in the presence or absence of 40 μg/mL TBZ or 60 μg/mL TBZ. All plates were incubated for 5 days at 30˚C. (B) *S. cerevisiae* AH109 strain was co-transformed with pGBKT7-derived plasmid and pGAD424-derived plasmid and selected on SC lacking leucine and tryptophan (SC-LW). Transformed cells were cultured and the cell suppression was spotted as described in Fig. 3-2B. All plates were incubated for 3 days at 30˚C.

Discussion

It has been reported that Pka1 is involved in glucose repression, chronological aging, regulation of transit from mitosis to meiosis, and stress response to KCl and $CaCl_2$ in *S. pombe* [33,39,43–47]. Pka1 also regulates the transition from the G2 phase to M phase, as the overexpression of Pka1 also causes growth defect and mitotic defects leading to cell elongation and DNA content accumulation [66]. On the other hand, PKA regulates the transition of G1/S phase in *S. cerevisiae* and the progression of G2/M phase in *Xenopus laevis* [67,68]. These reports suggest that PKA regulates cell cycle progression at several phases. However, its detailed mechanism is mostly unclear. In the M phase, *S. pombe* Pka1 is involved in the regulation of the anaphase-promoting complex (APC), but its detailed mechanism has not been elucidated [69–73]. In this study, the author and Yamaga found that *pka1*Δ exhibits the TBZ-sensitive phenotype and abnormal chromosome segregation in the presence of TBZ. In general, microtubule-destabilizing drugs inhibit the progression of the M phase in the cell cycle. Spindle assembly checkpoint (SAC) proteins such as Mad1, Mad2, Mad3, Bub1, Bub3, and Mph1 are not essential for the growth under normal condition. However, inactivated SAC causes the TBZ-sensitive phenotype and chromosome mis-segregation in the presence of microtubule destabilization drug [74]. SAC proteins negatively regulate APC for progression from metaphase to anaphase in the M phase. These results and the authors observation, that the *pka1*Δ strains exhibit the TBZ-sensitive phenotype and chromosome mis-segregation, together suggest that Pka1 regulates SAC and/or APC in the M phase.

To know how Pka1 regulates chromosome segregation, Yamaga performed multi-copy suppressor screening and isolated Mal3 (MAPs and +TIP protein) based on its ability to suppress TBZ sensitivity in the *pka1*Δ strains. The CH domain (1–143) of Mal3, but not other domains, is responsible for this suppression. The authors results suggest that the deletion of the *pka1* gene prevents the attachment of chromosome to the microtubule and the CH domain of Mal3 enhances the binding stability between the microtubule and chromosome. In fact, a microtubule unattached form of Mal3 (1–143 Q89E) failed to restore the sensitive of TBZ in the *pka1*Δ strains (Fig. 3-3A). The loss of functional Dis1, a TOG/XMAP215 microtubule plus end tracking polymerase, resulted in chromosome mis-segregation [75]. Leucine 841 and proline 844 of Dis1 at C-terminus are responsible for binding to Mal3, while the C-terminus region from 174 to 247 amino acids residue containing a part of coiled-coil domain and EB1 domain of Mal3 are required for binding with Dis1 [29]. Based on their report, the author suggests that the function of Dis1 is not required for the suppression of the TBZ-sensitive phenotype in the *pka1*Δ strain. The CH domain of Mal3 (1–143) did not localize to the microtubules during interphase and only localized to the microtubules during prophase to anaphase. The +TIP proteins, Tea1, Tea2, and Tip1, mostly play a role of in the cell polarity of microtubules in interphase [24]. Tea1, Tea2, and Tip1 bind through Mal3 to the microtubules

[24]. This is because the formation of +TIP complex mediated by EB1 domain of Mal3 is required to attach to microtubules in interphase, and the CH domain alone is not able to play this role as observed in the case of Tea1, Tea2, and Tip1 [24,76]. Therefore, the function of mitotic microtubules is important for suppression of the TBZ-sensitive phenotype in the *pka1*Δ strain. Overexpression of Alp14, which is a microtubule binding protein containing the TOG domain, functions similar to the CH domain of Mal3, but failed to restore the TBZ sensitive phenotype in the *pka1*Δ, indicating that the CH domain of Mal3 is required for microtubule stability in the *pka1*Δ strains [77]. The CH domain of Mal3 does not show discernible differences from the TOG domain regarding the Pka1-mediated microtubule stabilization.

Beinhauer *et al.* have shown that the *mal3*Δ strain exhibited the TBZ-sensitive phenotype and chromosome mis-segregation [23]. These results were also supported in this study (Fig. 3-1D and 3-5). The CH domain of Mal3 (1–143) is sufficient to suppress these phenotypes, while an unbinding form of Mal3 (1–143 Q89E) failed to reverse the TBZ sensitive phenotype of the *mal3*Δ strains (Fig. 3-5 and Table 3-3). These results indicate that the microtubule binding ability of Mal3 is important for proper function. It has been reported that the CH domain of Mal3 binds to microtubules in vitro [31], but function of the CH domain has not been clearly understood in vivo. The authors result in this study showed that the CH domain of Mal3 co-localizes with the microtubules and retains a role required for the proper segregation of chromosome. It has also been shown that the Mal3 (Q89R) mutant strongly binds to the microtubules and causes hyper phosphorylation at serine and threonine between 144 and 155 amino acids [30]. Overexpression of Mal3 (full-length Q89R) exhibited severe growth defect even under normal growth condition, probably due to excessive binding to microtubule; whereas overexpression of Mal3 (full-length Q89E) showed suppressive effect on the TBZ-sensitive phenotype of the *pka1*Δ and *mal3*Δ strains; even the mutant has only weak microtubule binding ability, probably due to the moderate effect of this mutation. Intriguingly, the effect of Q89 mutation was different when a truncated version of Mal3 was expressed. While Mal3 (1–143 Q89R) suppressed the TBZ-sensitive phenotype of the *pka1*Δ and *mal3*Δ strains, Mal3 (1–143 Q89E) failed to do so. This suggests that Mal3 (1–143 Q89E) does not have sufficient microtubule binding ability comparing with Mal3 (full-length Q89E) when overexpressed. The author also observed that the overexpression of Mal3 (1–241) causes sever growth inhibition compared to full-length Mal3 and other Mal3 fragmented proteins (Fig. 3-2C and 3-5A). These results suggest that the growth inhibition is caused by overexpression of fragments, including both the CH domain and the EB1 domain. The analysis to understand the cause of the severe growth inhibition observed with the truncated C-terminus mutant is currently underway. Genetic analysis on the *pka1*Δ and *mal3*Δ mutants suggest that these two genes work in parallel pathway, because the *pka1*Δ *mal3*Δ double mutant exhibited much severe sensitivity to TBZ than each single mutant (Fig. 3-1D). Overexpression of Pka1 did not rescue the TBZ-sensitive phenotype

of *mal3*Δ (Fig. 3-1H), supporting the idea that Mal3 operates downstream of the cAMP/PKA pathway during mitosis. In fact, the gain of functional PKA mutant, the *cgs1*Δ strain, rescued the TBZ sensitivity in the *cyr1*Δ strain (Fig. 3-1B) and exhibited the TBZ-tolerance phenotype compared to the wild type strain (Fig. 3-1D). This result suggests that the PKA activity is important for the response to the microtubule-destabilizing drugs.

Finally, the author showed that the functional suppression is also observed in the EB1 orthologs *S. cerevisiae* Bim1p (ScEB1), human EB1 (HsEB1), mouse EB1 (MmEB1), and *A. thaliana* EB1a (AtEB1a), in the *pka1*Δ and *mal3*Δ strains. EB1 protein has the CH domain at the N-terminus and EB1 domain at the C-terminus. In all these organisms, the EB1 protein binds to the microtubules and plays the role of microtubule stabilization [22]. The author identified that the EB1 proteins is responsible for proper chromosome segregation by genetic analysis. The authors complementation analysis indicates that the function of Mal3 is mostly conserved from yeasts to high eukaryotes, as the overexpression of AtEB1b and AtEB1c did not suppress the TBZ-sensitivity of the *pka1*Δ and *mal3*Δ strains (Fig. 3-3B). Because AtEB1c has a tail region with patches of basic amino acid residues, its function and structure are different from Mal3, budding yeast Bim1p (ScEB1), mouse EB1 (MmEB1), human EB1 (HsEB1), and AtEB1a [54]. The authors suppression results suggest that the function is conserved in fission yeast Mal3, budding yeast Bim1p (ScEB1), mouse EB1 (MmEB1), human EB1 (HsEB1), and *A. thaliana* AtEB1a. However, the author has no explanation on why the overexpression of AtEB1b failed to suppress the TBZ-sensitive phenotype in the *pka1*Δ and *mal3*Δ strains.

In conclusion, in addition to the known roles of Pka1 in meiosis, gluconeogenesis, chorological aging, and stress response of *S. pombe*, the author propose that Pka1 is also involved in the regulation of chromosome segregation during mitosis. The authors findings provide new insights into the novel function of Pka1 in regard to the CH domain of Mal3, in the regulation of microtubule organization and chromosome segregation in *S. pombe*.

Chapter 4

Glucose limitation and *pka1* deletion rescue aberrant mitotic spindle formation induced by Mal3 overexpression in *Schizosaccharomyces pombe*

Introduction

The EB1 family of proteins, commonly known as microtubule-associated proteins (MAPs), is conserved in eukaryotes ranging from yeast to human. EB1 proteins have several important roles in cellular functions, such as in promotion of microtubule polymerization, regulation of cell polarity, and stabilization of proper chromosome segregation [5,6]. In the fission yeast, *S. pombe*, EB1 protein Mal3 mainly regulates cell polarity by maintaining proper formation of microtubules and actin during interphase, and also by ensuring appropriate chromosome segregation by regulating microtubule-chromosome attachment in mitosis [6,23,25]. Mal3 interacts with several proteins, including CLIP-170/Tip1 and kinesin/Tea2 in interphase, and blinkin/Spc7 and TOG/Dis1 in mitosis [24,28,29]. However, details regarding the mitotic function of Mal3 are mostly unclear. Mal3 has two major domains: the Calponin homology (CH) domain at the N-terminus and the end-binding (EB1) domain at the C-terminus [62,78]. The CH domain promotes microtubule polymerization, but its [6,23,25]mechanism is also unclear [65]. The EB1 domain mediates interactions between binding partners, such as EB1/Mal3, CLIP-170/Tip1, and CLASP1/Peg1 [5]. Two Mal3 mutants, Mal3 (K63D) and Mal3 (Q89E), that fail to bind microtubules *in vitro* have been isolated [31], and another, Mal3 mutant (Q89R), was found to have excessive binding activity to microtubules, both *in vivo* and *in vitro* [30,31].

The kinesin-5 family of proteins is responsible for establishing bipolar spindles in many organisms [13,79–83], and inhibition of kinesin-5 activity results in monopolar spindle formation and chromosome mis-segregation [83]. In *S. pombe*, kinesin-5 is encoded by the *cut7* gene, which is essential gene for growth [13]. A temperature sensitive *cut7-446* mutant strain exhibits growth defects, abnormal chromosome segregation (the *cut* phenotype), and monopolar spindle formation at high temperatures [13,19,74]. Notably, *mal3*Δ strains rescued the temperature sensitive phenotype of the *cut7-22* mutant [19].

The cAMP/PKA pathway is known as a major glucose response pathway in yeasts [84–87]. In *S. pombe*, the cAMP/PKA pathway consists of the G protein-coupled receptor Git3, as well as a heterotrimeric G protein alpha subunit (Gpa2), a beta subunit (Git5), a gamma subunit (Git11), an adenylate cyclase (Cyr1), a protein kinase A regulatory subunit (Cgs1), and a protein kinase A catalytic subunit (Pka1) [33,37,39–42,44]. This pathway has roles in glucose-sensing, regulation of transition to meiosis, chronological aging, stress response, and regulation of proper chromosome segregation [33,39,43–47,88]. The author have recently reported that the *pka1*Δ strains exhibit a TBZ-sensitive phenotype and chromosome mis-segregation. These phenotypes were suppressed by overexpression of Mal3, and the ability of Mal3 to bind microtubules was an important part of these effects [88]. The author have also shown that deletion of *pka1* rescued growth defects caused by Mal3-overexpression in the wild-type strain, but detailed mechanistic analysis has not been conducted [88].

In this study, the author showed that Mal3 overexpression induced monopolar spindle formation in addition to the growth inhibition, and these effects were suppressed by the deletion of *pka1* and by glucose limitation. The author also showed that deletion of *pka1* and glucose limitation rescued the temperature sensitive phenotype and monopolar spindle formation in the *cut7-446* mutant. As glucose limitation masks Pka1 activity by the formation of the Pka1-Cgs1 complex [89], the glucose-Pka1 signaling pathway somehow controls microtubule organization. This likely occurs either through direct or indirect involvement of a microtubule-associated protein, such as Mal3.

Results

Overexpression of Mal3 induces monopolar spindle formation

Overexpression of Mal3 causes growth defects in wild-type cells [23]. To confirm this phenotype, wild-type cells were transformed with pREP3x (empty vector) or pREP3x-mal3. Mal3-overexpressing cells exhibited growth defects (Fig. 4-1A) as described previously [23]. FACS analysis of Mal3-overexpressing cells showed that the number of cells with mitotic defects, as indicated by the presence of 4C DNA content and chromosome mis-segregation, was significantly increased (Fig. 4-1B and 4-1C). Since Mal3-overexpression caused mitotic defects, the author next observed microtubules, by GFP-Atb2, and spindle pole bodies (SPB), by Sad1-mRFP. Around 25% of Mal3-overexpressing cells formed monopolar spindles, observed as a V-shape (Fig. 4-1D and 4-1E). The author confirmed that Mal3-overexpression did not significantly affect the protein expression level of α-tubulin (Fig. 4-1D). The author then used the *nmt41* promoter, which is a weaker promoter than the *nmt1* promoter, to govern the expression of Mal3 to test monopolar spindle formation. Mal3-overexpression under the *nmt41* promoter showed normal spindle formation, although cells were elongated (Fig. 4-1D). Therefore, only a high level of Mal3 expression caused the monopolar spindle formation.

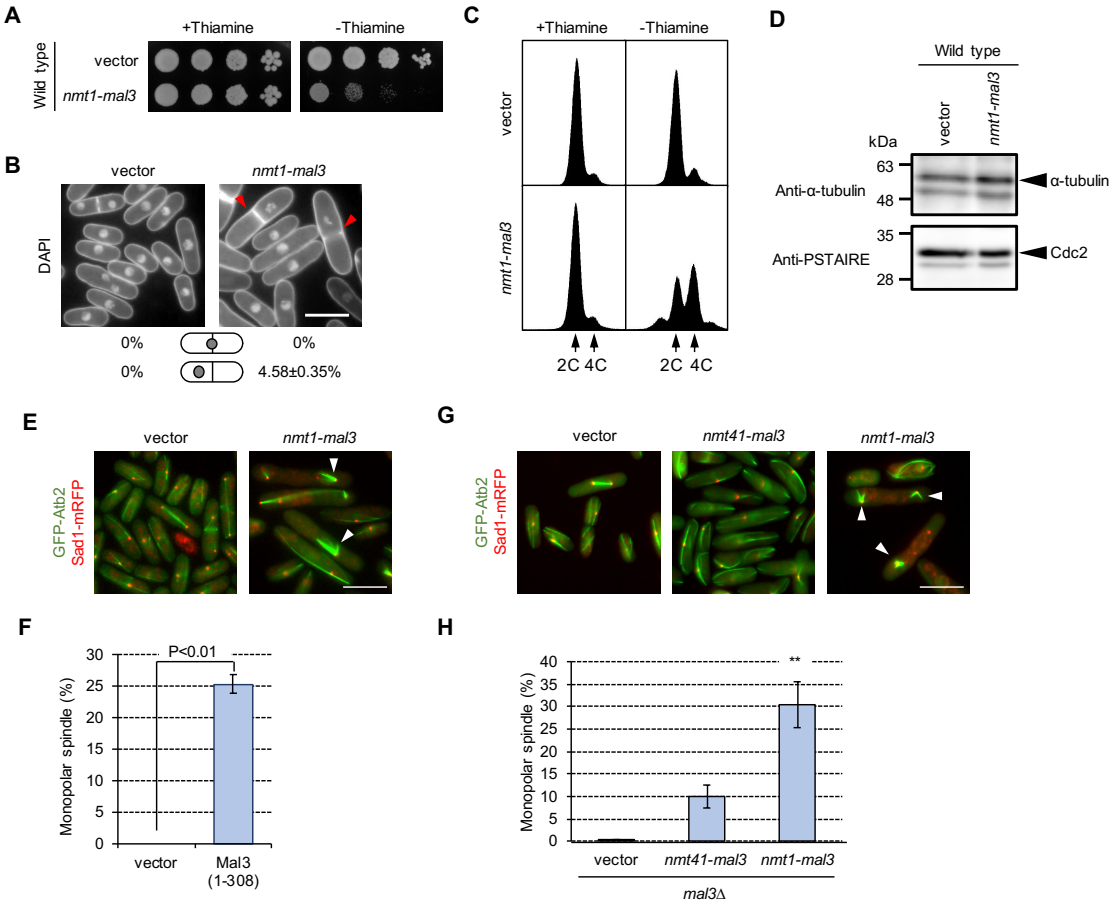

Fig. 4-1. Overexpression of Mal3 causes a growth defect, accumulation of 4C DNA, and monopolar spindle formation.

(A) Wild-type (PR109) cells harboring pREP3X (vector) or pREP3X-mal3 (1-308; full-length) were cultured for 1 day on EMMU containing 15 µM thiamine at 30˚C to repress expression of the *mal3* gene from the *nmt1* promoter. Cells were spotted onto EMMU (2% glucose) in the presence or absence of 15 µM thiamine. All plates were incubated for 4 days at 30˚C. (B) Cells were stained with DAPI to visualize the nuclei and septum. Red arrowheads indicate chromosome mis-segregation. Scale bar: 10 µm. (C) FACS profile of cells overexpressing Mal3. Cells were fixed and stained with propidium iodide. (D) Whole-cell extracts were prepared from the wild type (PR109) harboring pREP3X and wild type harboring pREP3X-Mal3 (1-308) strains. α-tubulin was detected by anti-α-tubulin antibody. Anti-PSTAIRE was used as an internal loading control. Monopolar spindle formation is dependent on the level of Mal3 expression. (E) A GFP-Atb2 (green color) and Sad1-mRFP (red color) expressing strain (TTP76) harboring pREP3X (vector) or pREP3X-mal3 (1-308; full-length); Atb2 localizes to microtubules and Sad1 localizes to spindle pole body which is similar to the centrosome in mammals. Sad1-mRFP was used to visualize the end of microtubules. Arrowheads indicate monopolar spindles. Scale bar: 10 µm. (F) Enumeration of monopolar spindle formation in the transformants. Approximately 200 cells were analyzed in each strain. Experiments were performed three times; averages with S.D. are shown. (G) A GFP-Atb2 (green color) and Sad1-mRFP (red color) strain (TTP76) harboring pREP3X (vector), pREP3X-mal3 (1-308; full-length), or pREP41X-mal3 (1-308; full-length) was cultured and observed by fluorescent microscopy. Arrowheads indicate monopolar spindles. Scale bar: 10 µm. (H) Enumeration of monopolar spindle formation in the transformants. Approximately 200 cells were analyzed in each strain. Experiments were performed three times; averages with S.D. are shown. Double asterisk (**) indicates P-value < 0.01 compared with the TTP76 strain harboring pREP41X-mal3 (*nmt41-mal3*).

Overexpression of the Mal3 CH with the EB1 domain causes monopolar spindle formation

Since Mal3 has two major domains, namely, the Calponin homology (CH) domain for microtubule binding at the N-terminus (3-103) and the end-binding (EB1) domain for binding with other proteins at the C-terminus (197-241), the author analyzed which domain caused growth defects and monopolar spindle formation in Mal3-overexpressing cells. To do so, the author used five plasmids that included different portions of the fragmented Mal3. The *mal3*Δ mutant was transformed with each plasmid, incubated in the absence of thiamine to induce the *mal3* expression, and cells were spotted onto EMMU in the presence or absence of thiamine. Overexpression of Mal3 (1-308) or Mal3 (1-241) resulted in growth defects, whereas Mal3 (1-197), Mal3 (135-241), and Mal3 (135-308) showed normal growth (Fig. 4-2A). FACS analysis of Mal3 (1-308) and Mal3 (1-241) overexpressing cells showed 4C DNA content (Fig. 4-2B) and a substantial frequency of monopolar spindles was noted in microscopic analysis (Fig. 4-2C and 4-2D). The protein expression levels of the Mal3 fragments were not different from the full length Mal3 (Fig. 4-2E). These results suggest that the combination of the Mal3 CH and the EB1 domains is responsible for defective growth and monopolar spindle formation in the Mal3-overexpressing cells.

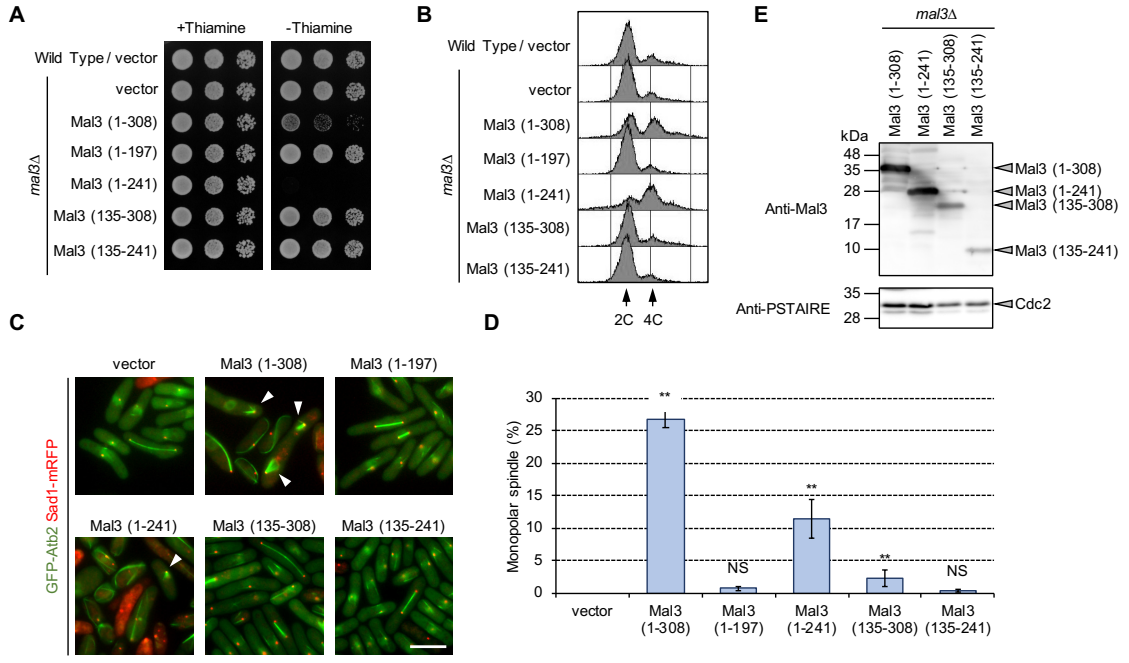

Fig. 4-2. Overexpression of the CH and EB1 domain of Mal3 causes growth defects, accumulation of 4C DNA content, and monopolar spindle formation.

(A) Wild-type (PR109) and *mal3*Δ (TTP1) strains harboring pREP3X (vector), pREP3X-mal3 (1-308: full-length), pREP3X-mal3 (1-197), pREP3X-mal3 (1-241), pREP3X-mal3 (135-308), or pREP3X-mal3 (135-241) were cultured and spotted onto EMMU (2% glucose) in the presence or absence of 15 μM thiamine. All plates were incubated for 4 days at 30˚C. (B) FACS analysis of 2C and 4C DNA contents in the transformants. (C) A GFP-Atb2 (green color) and Sad1-mRFP (red color) expressing strain (TTP171) harboring pREP3X (vector), pREP3X-mal3 (1-308: full-length), pREP3X-mal3 (1-197), pREP3X-mal3 (1-241), pREP3X-mal3 (135-308), or pREP3X-mal3 (135-241). Arrowheads indicate monopolar spindles. Scale bar: 10 μm. (D) Enumeration of monopolar spindle formation in the transformants. Approximately 200 cells were analyzed in each strain. Experiments were performed three times;

averages with S.D. are shown. Double asterisks (**) indicate P-value < 0.01 compared with the TTP76 strain harboring pREP3X (vector). NS indicates no significant difference with the TTP76 strain harboring pREP3X (vector). (E) Mal3 protein was detected using an anti-Mal3 antibody. Anti-PSTAIRE was used as an internal loading control.

Microtubule binding by the Mal3 CH domain is required for monopolar spindle formation

The author next investigated whether microtubule binding ability of Mal3 is responsible for the observed growth defects and monopolar spindle formation using the Mal3 (Q89R) and Mal3 (Q89E) mutant. The Mal3 (Q89R) mutant strongly binds to the microtubules but the Mal3 (Q89E) mutant does not [30,31]. Overexpression of the Mal3 (Q89R) mutant resulted in growth defects, whereas overexpression of the Mal3 (Q89E) mutant did not affect growth (Fig. 4-3A). Interestingly, the Q89E mutation in Mal3 (1-241) abolished the defective growth phenotype (Fig. 4-3A), indicating that microtubule binding is important for causing the growth defects in Mal3-overexpressing cells. The author also noted that the Mal3 (Q89R) mutant had an increased amount of 4C DNA cells than Mal3 (1-308), and a substantial frequency of monopolar spindle formation, similar to Mal3 (1-308) (Fig. 4-3B-D). Because a point mutation in Mal3 (Q89E) does not completely abolish microtubule binding by the CH domain, the Mal3 (Q89E) mutant showed a lower, but nonzero, frequency of monopolar spindle formation (Fig. 4-3D). The Q89E mutation in Mal3 (1-241) also resulted in reduced 4C DNA contents and monopolar spindle formation (Fig. 4-3B-D). The author confirmed protein levels of Mal3 and its derivatives were not different among Mal3 (1-308), Mal3 (1-241), Mal3 (Q89R), and Mal3 (Q89E) (Fig. 4-3E). These results suggest that microtubule binding by the CH domain contributes to the defective growth phenotype and to monopolar spindle formation in Mal3-overexpressing cells.

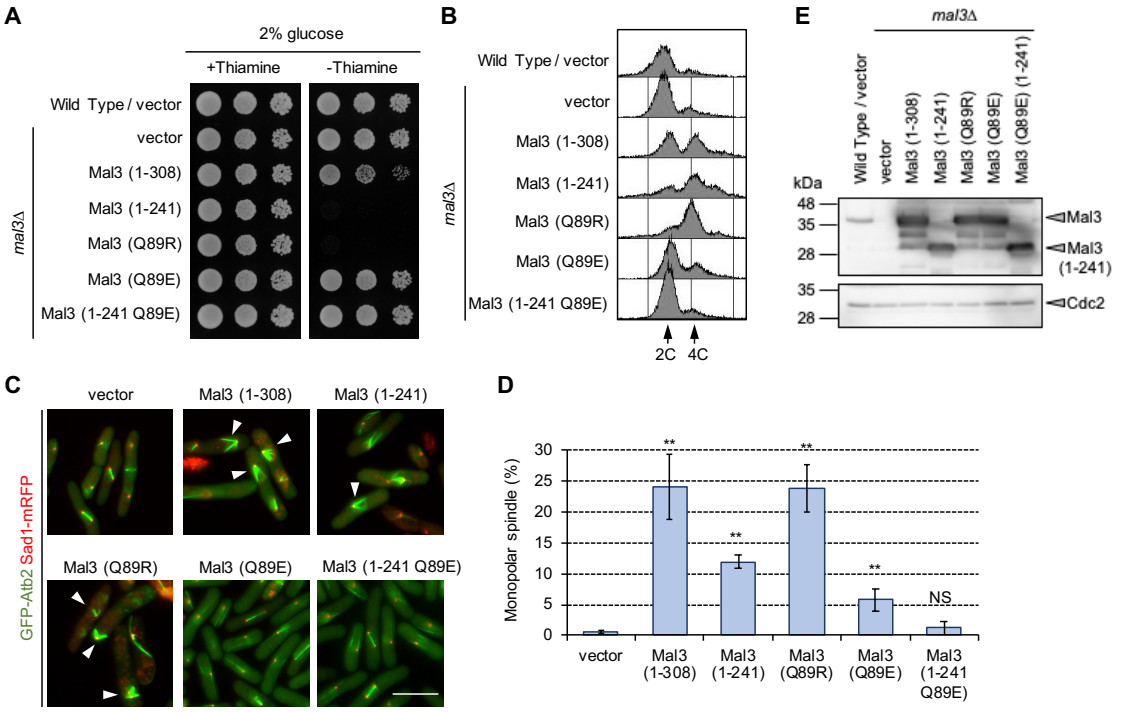

Fig. 4-3. Microtubule binding of Mal3 causes growth defects, accumulation of 4C DNA, and monopolar spindle formation.

(A) Wild-type (PR109) and *mal3*Δ (TTP1) strains harboring pREP3X (vector), pREP3X-mal3 (1-308: full-length), pREP3X-mal3 (1-241), pREP3X-mal3 (Q89R), pREP3X-mal3 (Q89E), or pREP3X-mal3 (1-241 Q89E) were cultured and spotted onto EMMU (2% glucose) in the presence or absence of 15 µM thiamine. All plates were incubated for 4 days at 30˚C. (B) 2C and 4C DNA content of transformants were analyzed by FACS. (C) GFP-Atb2 (green color) and Sad1-mRFP (red color) expressing strains (TTP171) harboring pREP3X (vector), pREP3X-mal3 (1-308: full-length), pREP3X-mal3 (1-241), pREP3X-mal3 (Q89R), pREP3X-mal3 (Q89E), or pREP3X-mal3 (1-241 Q89E) were cultured and observed by fluorescent microscopy. Arrowheads indicate monopolar spindles. Scale bar: 10 µm. (D) Enumeration of monopolar spindle formation in the transformants after 24 h incubation without thiamine. Approximately 200 cells were analyzed in each strain. Experiments were performed three times; averages with S.D. are shown. Double asterisks (**) indicate P-value < 0.01 compared with the GFP-Atb2 Sad1-mRFP strain harboring pREP3X (vector). NS indicates no significant different with the GFP-Atb2 Sad1-mRFP strain harboring pREP3X (vector). (E) Mal3 protein was detected using an anti-Mal3 antibody. Anti-PSTAIRE was used as an internal loading control for Cdc2 protein.

Mal3 (1-241) and Mal3 (Q89R) reduce cell viability and cause high ratio of monopolar spindle formation at early time point

Since the frequency of monopolar spindle formation was higher in Mal3 (1-308) and Mal3 (Q89R) expressed cells than Mal3 (1-241) expressed cells (Fig. 4-3D), the author carefully examined the timing of cell viability loss and monopolar spindle formation in Mal3 (1-308), Mal3 (1-241) and Mal3 (Q89R) overexpressed cells. Overexpression of the Mal3 (1-241) and Mal3 (Q89R) mutants reduced cell viability at the earlier point than overexpression of Mal3 (1-308) (Fig. 4-4A). Monopolar spindle formation was substantially high (34-48%) at 18 h in Mal3 (1-241) and Mal3 (Q89R) overexpressed cells, then decreased after 24 h, whereas overexpression of Mal3 (1-308) remained at substantially high frequency (28%) at 24

h, then decreased at 30 h (Fig. 4-4B). Thus, expression of Mal3 (1-241) and Mal3 (Q89R) strongly induced monopolar spindle formation at the early stage.

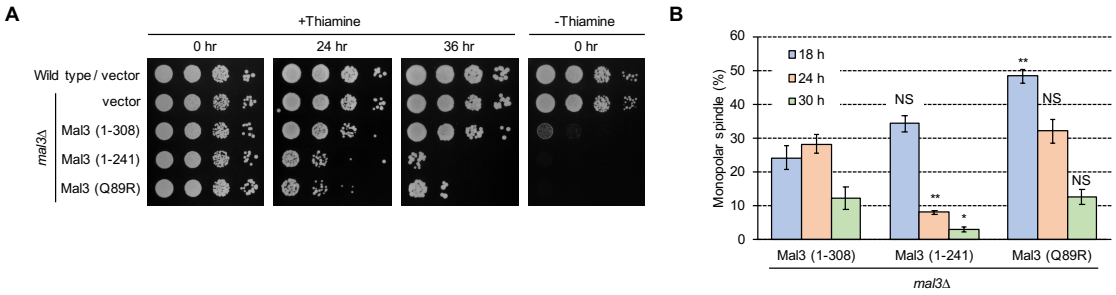

Fig. 4-4. Mal3 (1-241) and Mal3 (Q89R) immediately induce monopolar spindle formation.
(A) Cells were cultured in EMMU in the presence of 15 μM thiamine, washed out, resuspended into EMM without thiamine, incubated for 0, 24, and 36 h at 30˚C. Cells were spotted onto EMMU in the presence or absence of thiamine and incubated for 4 days at 30˚C. (B) Enumeration of monopolar spindle formation in the transformants. Approximately 200 cells were analyzed in each strain. Experiments were performed three times; averages with S.D. are shown. Double asterisks (**) and asterisk (*) indicate P-value < 0.01 and P<0.05 compared with the GFP-Atb2 Sad1-mRFP strain harboring pREP3X-mal3 (1-308) at each time point. NS indicates no significant different with the GFP-Atb2 Sad1-mRFP strain harboring pREP3X-mal3 (1-308).

Loss of functional PKA rescues growth defects and monopolar spindle formation

The author have previously reported that overexpression of Mal3 rescues the TBZ-sensitive phenotype of the *pka1*Δ mutant [88]. The author have also shown that the *pka1*Δ mutant grows normally when overexpressing Mal3 (1-308; full-length), but showed growth defects from Mal3 (1-241) or Mal3 (Q89R)-overexpression [88]. To test the relevance of Pka1 in the phenotypes observed in this current study, the *pka1*Δ mutant harboring pREP3X or pREP3x-mal3 was spotted onto EMMU plates and the DNA contents of each transformant in the absence of thiamine was analyzed. The *pka1*Δ mutant did not exhibit the defective growth phenotype and had lower 4C DNA contents in Mal3-overexpressing cells than were observed in wild-type cells (Fig. 4-5A and 4-5B). The author also analyzed the phenotypes in *cyr1*Δ and *cgs1*Δ strains because deletion of *cyr1* results in Pka1 inactivation and deletion of *cgs1* results in constitutive activation of Pka1[33,39,43–47,88]. The author found that the *cyr1*Δ strain rescued the growth defects in Mal3-overexpressing cells but the *cgs1*Δ strain showed more severe growth defects (Fig. 4-5C), indicating that Pka1 activity is highly related to the suppressive effects of defective growth in Mal3-overexpressing cells. The frequency of monopolar spindle was significantly decreased in the *pka1*Δ mutant (Fig. 4-5D and 4-5E), further suggesting that Pka1 is involved in the regulation of appropriate mitotic spindle formation.

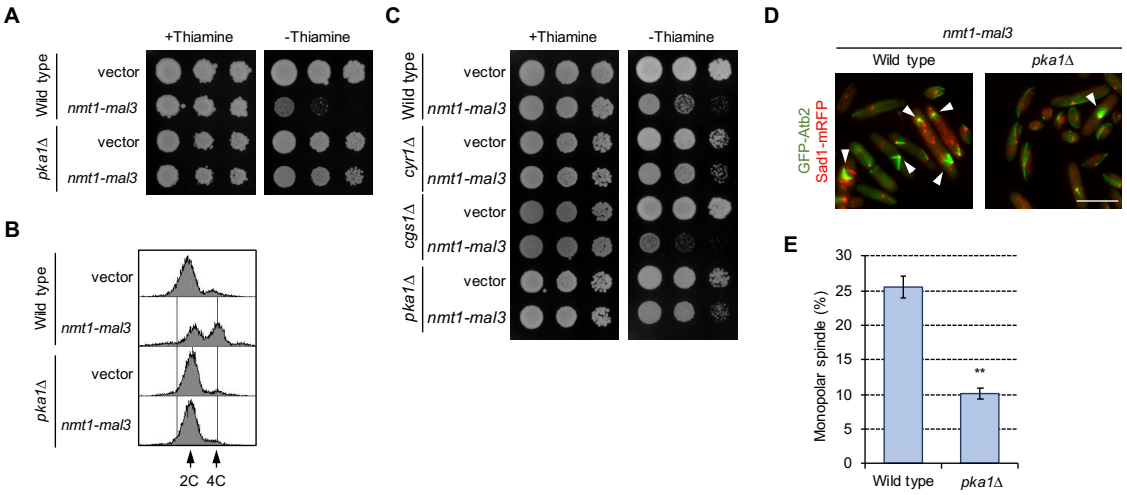

Fig. 4-5. The *pka1*Δ strain rescues growth defects, accumulation of 4C DNA, and monopolar spindle formation in Mal3-overexpressing cells.

(A) Wild-type (PR109) and *pka1*Δ (YMP36) strains harboring pREP3X (vector) or pREP3X-mal3 (1-308: full-length) were cultured and spotted onto EMMU (2% glucose) in the presence or absence of 15 μM thiamine. All plates were incubated for 4 days at 30˚C. (B) 2C and 4C DNA content of transformants were analyzed by FACS. (C) Wild-type (PR109), *cyr1*Δ (YMP28), *cgs1*Δ (YMP40), or *pka1*Δ (YMP36) strains harboring pREP3X (vector) or pREP3X-mal3 (1-308; full-length) were cultured and spotted onto EMMU (2% glucose) in the presence or absence of thiamine. All plates were incubated for 4 days at 30˚C. (D) The GFP-Atb2 (green color) and Sad1-mRFP (red color) expressing strain (TTP76) and *pka1*Δ GFP-Atb2 Sad1-mRFP (TTP218) strains harboring pREP3X (vector) or pREP3X-mal3 (1-308: full-length) were cultured and observed by fluorescent microscopy. Arrowheads indicate monopolar spindles. Scale bar: 10 μm. (E) Enumeration of monopolar spindle formation in the transformants. Approximately 200 cells were analyzed in each strain. Experiments were performed three times; averages with S.D. are shown. Double asterisk (**) indicates P-value < 0.01 compared with the TTP76 strain harboring pREP3X (vector).

Glucose limitation rescues growth defects and abnormal spindle formation

Since the cAMP/PKA pathway is a known glucose response pathway, the author next investigated whether glucose concentration affected growth defects and monopolar spindle formation in Mal3-overexpressing cells. Mal3 (1-308; full-length)-overexpressing cells grew normally on glucose-limited medium (0.1% glucose) (Fig. 4-6A), notably different from the defective growth observed on normal glucose medium (3% glucose) (Fig. 4-2A). However, cell growth on glucose-limited medium was inhibited in Mal3 (1-241)- or Mal3 (Q89R)-overexpressing cells (Fig. 4-6A), which had more severe phenotype compared to that of Mal3 (1-308). The author next analyzed the DNA content of Mal3-overexpressed cells under glucose-limited conditions (0.1% glucose). Accumulation of 4C DNA in Mal3 (1-308; full-length)-, Mal3 (1-241)-, and Mal3 (Q89R)-overexpressing cells (Fig. 4-6B) was reduced under glucose-limiting conditions (0.1% glucose). The monopolar spindle formation phenotype induced by Mal3 (1-308; full-length) was rescued under glucose-limiting conditions, whereas the same phenotype was not rescued by glucose limitation in Mal3 (1-241) or Mal3 (Q89R) expressing cells (Fig. 4-6C and 4-6D). These results

indicate that glucose limitations partially antagonize the growth defect and monopolar spindle formation in Mal3-overexpressed cells.

Because the TORC2 and AMPK pathways are also glucose response pathways in *S. pombe* [90,91], the author next investigated whether a *tor1*Δ or *ssp2*Δ strain rescues defective growth in Mal3-overexpressing cells. The growth defects caused by Mal3-overexpression were not rescued in the *tor1*Δ and *ssp2*Δ strains under normal glucose conditions (3% glucose) (Fig. 4-6E), indicating that only the cAMP/PKA pathway is regulating the growth and monopolar spindle formation in Mal3-overexpressing cells.

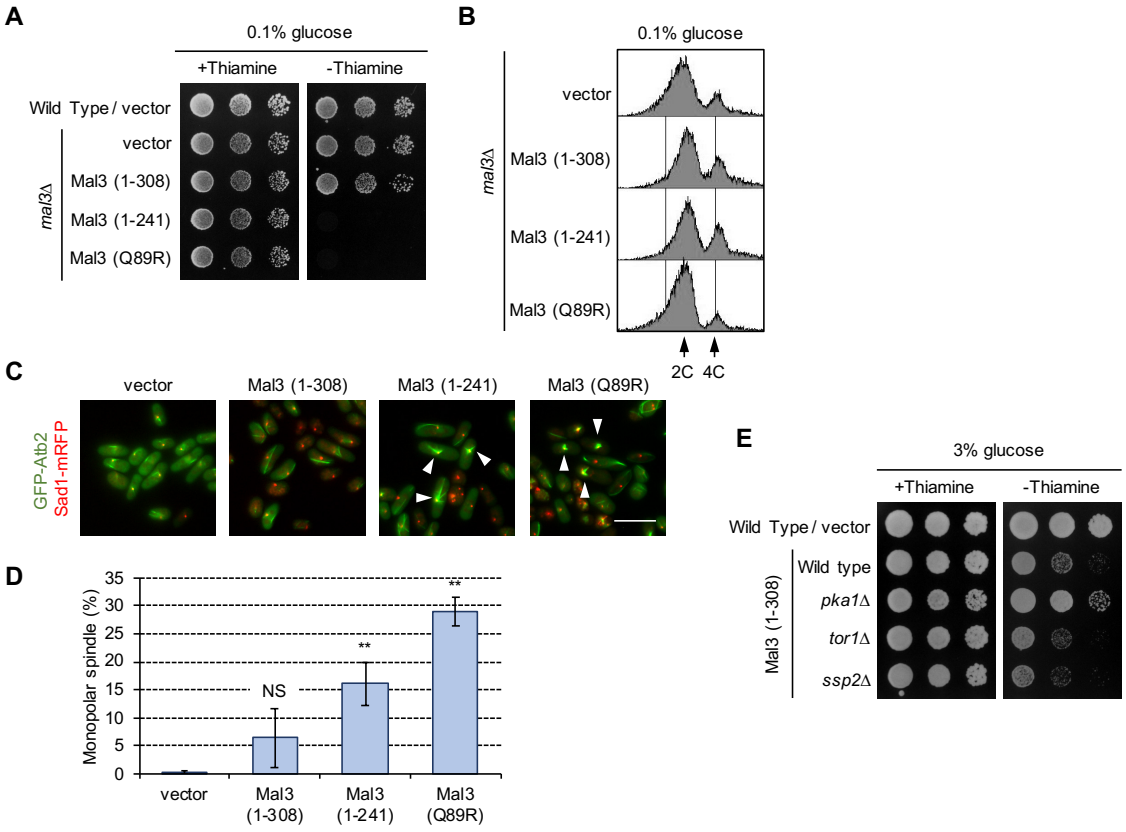

Fig. 4-6. Glucose limitation rescues the Mal3-overexpression phenotype.

(A) Wild-type (PR109) and *mal3*Δ (TTP1) strains harboring pREP3X (vector), pREP3X-mal3 (1-308: full-length), pREP3X-mal3 (1-241), or pREP3X-mal3 (Q89R) were cultured and spotted onto EMMU glucose-limiting medium (0.1% glucose) in the presence or absence of 15 μM thiamine. All plates were incubated for 4 days at 30˚C. (B) Transformants were cultured into EMMU containing 15 μM thiamine at 30˚C. Cells were washed, transferred into EMMU glucose-limited medium (0.1% glucose) without thiamine, and incubated for 24 h at 30˚C. Cells were fixed and stained with propidium iodide. (C) The GFP-Atb2 (green color) and Sad1-mRFP (red color) expressing strain (TTP171) harboring pREP3X (vector), pREP3X-mal3 (1-308: full-length), pREP3X-mal3 (1-241), and pREP3X-mal3 (Q89R) were cultured in EMMU glucose-limiting medium (0.1% glucose) and observed by fluorescent microscopy. Arrowheads indicate monopolar spindles. Scale bar: 10 μm. (D) Enumeration of monopolar spindle formation in the transformants. Approximately 200 cells were analyzed in each strain. Experiments were performed three times; averages with S.D. are shown. Double asterisks (**) indicate P-value < 0.01 compared with the TTP171 strain harboring pREP3X (vector). NS indicates no significant difference with the TTP171 strain harboring pREP3X (vector). (E) Wild-type (PR109), *pka1*Δ (YMP36), *tor1*Δ (TTP233), and *ssp2*Δ (MBY1748) strains harboring pREP3X (vector) or pREP3X-mal3 (1-308: full-length) were cultured and spotted onto EMMU (3% glucose) in the presence or absence of 15 μM thiamine. All plates were incubated for 4 days at 30˚C.

The *cut7-446* mutant is rescued by loss of functional PKA and glucose limitations

The *cut7-446* mutant has previously been shown to exhibit monopolar spindle formation [13] as was observed in Mal3-overexpressing cells, and the temperature sensitive phenotype in *cut7-22* was rescued by *mal3* deletion [19]. Based on these observations, the author investigated genetic interactions between the *cut7-446* mutant and the *pka1*Δ strain and the effects of glucose limitation. The temperature sensitive phenotype of the *cut7-446* mutant was partially rescued at 30˚C by *pka1* deletion (Fig. 4-7A) and by glucose-limitation (Fig. 4-7B). Monopolar spindle formation was also abolished by *pka1* deletion and glucose limitation at semi-restriction temperature (30˚C) in the *cut7-446* mutant (Fig. 4-7C and 4-7D). The *cut7-446* mutant showed higher DNA contents than 4C by FACS analysis (Fig. 4-7E). However, the *cut7-446* mutant exhibited monopolar spindle formation at a restrictive temperature, 37˚C, from deletion of *pka1* or limited glucose (Fig. 4-7F). Thus, loss of functional Pka1 and glucose limitation partially rescues growth defects and monopolar spindle formation in the *cut7-446* mutant.

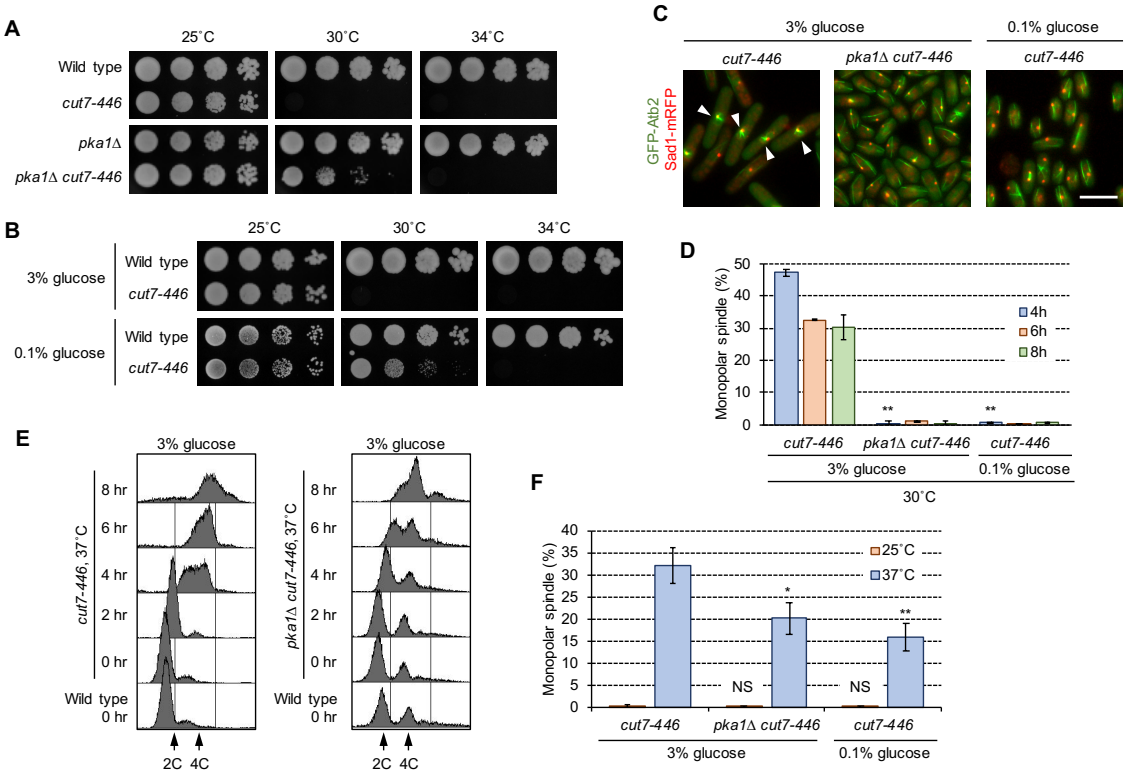

Fig. 4-7. The phenotypes of the *cut7-446* mutant are rescued by loss of functional Pka1 and under glucose-limiting conditions.

(a) Wild- type (PR109), *cut7-446* (YMP324), *pka1*Δ (YMP36), and *pka1*Δ *cut7-446* (YMP351) *S. pombe* strain were grown on YES, harvested, and cell suspensions were spotted on YES (3% glucose) plates. All plates were incubated for 4 to 5 days at indicated temperature (25 ˚C for 5 days; 30 ˚C for 4 days, and 34˚C for 4 days). (b) Wild-type (PR109) and *cut7-446* (YMP324) *S. pombe* strains were grown on YES, harvested, and cell suspensions were spotted on YES (3% glucose) and YES (0.1% glucose) plates. All plates were incubated for 4 to 7 days at indicated temperature (3% glucose 25 ˚C for 5 days; 3% glucose 30 ˚C for 4 days, 3% glucose 34˚C for 4 days, 0.1% glucose 25 ˚C for 7 days; 0.1% glucose 30 ˚C for 7 days, and 0.1% glucose 34˚C for 7 days). (c) The *cut7-446* GFP-Atb2 (green color) and Sad1-mRFP (red color) expressing strain (TTP157) and *pka1*Δ *cut7-446* GFP-Atb2 Sad1-mRFP

(TTP277) strains were cultured in EMMLU (3% glucose), washed three times with water, cultured in EMMLU (3% glucose) or EMMLU (0.1% glucose) medium for 6 h at 30°C and observed by fluorescent microscopy. Arrowheads indicate monopolar spindles. Scale bar: 10 μm. (d) Enumeration of monopolar spindle formation in the same cells. Approximately 200 cells were analyzed in each strain. Experiments were performed three times; averages with S.D. are shown. Double asterisks (**) indicate P-value < 0.01 compared with the *cut7-446* strain grown for 4 h. (E) FACS profile of the *cut7-446* mutant. Cells were incubated at 37˚C, fixed, and stained with propidium iodide. (F) The *cut7-446* GFP-Atb2 Sad1-mRFP (TTP157) and *pka1*Δ *cut7-446* GFP-Atb2 Sad1-mRFP (TTP277) strains were cultured to mid-log phase at 25 ˚C or for 6 h at 37 ˚C as described in Figure 7c. GFP-Atb2 (green color) and Sad1-mRFP (red color) were observed by fluorescent microscopy and monopolar spindle formation was enumerated. Approximately 200 cells were analyzed in each strain. Experiments were performed three times; averages with S.D. are shown. Double asterisk (**) and asterisk (*) indicate P-value < 0.01 and <0.05 compared with the *cut7-446* strain at 37˚C in 3% glucose. NS indicates no significant difference compared with the *cut7-446* strain at 25˚C in 3% glucose.

The *mal3* deletion did not suppress growth defect by overexpression of *klp2*, and overexpression Mal3 failed to suppress growth defect of *klp2*, *tip1*, and *ssm4* deletion strains.

Kinesin-14/Klp2, causes growth inhibition with monopolar spindle formation by its overexpression. Moreover, growth defect of the *cut7-22* mutant was suppressed by deletion of *klp2*[17]. Since Klp2 and Mal3 have been reported to interact each other [27], the author investigated whether Mal3 is involved in these phenotypes. As a result, growth inhibition due to Klp2 overexpression was not suppressed by the *mal3* deletion. Growth inhibition by Mal3 overexpression was not suppressed by the loss of functional Klp2.The EB1 family protein has an EEY/F motif at the tail, which is the binding site of the proteins harboring a CAP-glycine motif (GKNDG). In *S.pombe*, Tip1 and Ssm4 have the CAP-glycine motif (GKNDG). Therefore, the author investigated whether overexpression of Mal3 is suppressed by these deletions. As a result, overexpression of Mal3 was not suppressed by deletion of *tip1* and *ssm4*. These results suggested that Klp2, Tip1, and Ssm4 deletion don't affect growth defect by overexpression of Mal3.

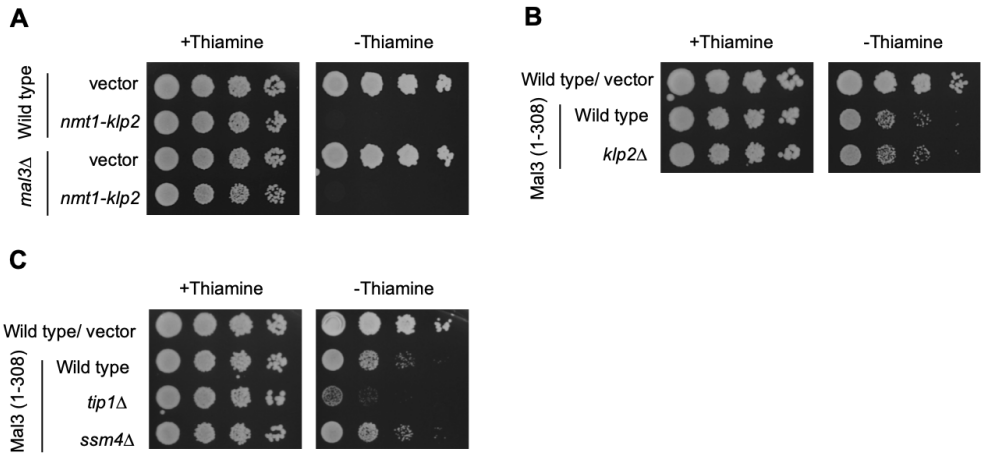

Fig. 4-8. The *mal3* deletion did not suppress growth defect by overexpression of *klp2*, and Klp2, Tip1, and Ssm4 deletion don't affect growth defect by overexpression of Mal3

(A) Wild-type (PR109) and *mal3*Δ (TTP1) strains harboring pREP3X (vector), pREP3X-klp2 were cultured and spotted onto EMMU (2% glucose) in the presence or absence of 15 μM thiamine. All plates were incubated for 4 days at 30˚C. (B) Wild-type (PR109) and *klp2*Δ (TTP254) strains harboring pREP4X (vector), pREP4X-mal3 (1-308: full-length) were cultured and spotted onto EMMU (2% glucose) in the presence or absence of 15 μM thiamine. All plates were incubated for 4 days at 30˚C. (C) Wild-type (PR109), *tip1*Δ (TTP223), and *ssm4*Δ (TTP224) strains harboring pREP3X (vector), pREP3X-mal3 (1-308: full-length) were cultured and spotted onto EMMU (2% glucose) in the presence or absence of 15 μM thiamine. All plates were incubated for 4 days at 30˚C.

Discussion

In this study, the author investigated the role of Mal3 in mitosis by observing the cellular effects of Mal3 overexpression. Overexpression of Mal3 resulted in a specific growth defect, increased 4C DNA contents, chromosome mis-segregation, and monopolar spindle formation (Fig. 4-1) as has been described previously [23]. Although microtubule dynamics are reportedly affected in Mal3-overexpressing cells [23], the detailed molecular mechanism underlying this has not been described. The authors findings in this study showed that overexpression of the CH domain (1-197) or the EB1 domain (135-308) alone did not result in defective growth or elevated monopolar spindle formation, and that the phenotypes caused by overexpression of Mal3 or Mal3 (1-241) were abolished by a mutation (Q89E) that renders the Mal3 protein unable to bind microtubules (Fig. 4-3). It has been shown that the CH domain contributes to microtubule binding and that the EB1 domain is involved in microtubule stability, proper chromosome segregation, and interactions with binding partners, such as Dis1/TOG, Tip1/CLIP-170, and Peg1/CLASP [22,24,27–31,76,88]. Based on these observations, results from the authors current study suggest that the EB1 domain is responsible for monopolar spindle formation when Mal3 binds to microtubules through the CH domain. Bipolar spindle formation might be controlled by microtubule dynamics or Mal3 binding partners mediated through the EB1 domain. One such binding partner, Klp2, causes monopolar spindle formation upon Klp2 overexpression [17]. Overexpression of Mal3 possibly recruits excess Klp2 around microtubules, which results in monopolar spindle formation similar to that observed from overexpression of Klp2. However, observed that *mal3* deletion did not rescue the growth defect caused by Klp2-overexpression and conversely *klp2* deletion did not rescue the growth defect caused by Mal3-overexpression (Fig.4-8A). These observations indicate that the growth inhibitory effect of Mal3-overexpression does not depend on Klp2 and suggest that Mal3-overexpression might cause monopolar spindle formation by regulating microtubule dynamics or through the effect of yet unidentified binding partner(s). In the authors findings, overexpression of a truncated Mal3 (1-241) exhibited more severe phenotype compared to the full-length Mal3 (1-308), consistent with the authors previous report [88]. These results suggest that the 241-308 region of Mal3 is required for proper chromosome segregation and might be responsible for viability or suppression of monopolar spindle formation. The EB1 family protein has an EEY/F motif at the tail, which is the binding site of the proteins harboring a CAP-glycine motif (GKNDG). *S. pombe* Mal3 has an ITF amino acid sequence at the tail which is thought to have a function similar to that of the EEY/F motif [21]. *S. pombe* has at least 3 proteins including Tip1 (CLIP-170), Ssm4 (dynactin), and Alp11 (tubulin chaperone cofactor B) that harbor the CAP-glycine motif according to the *S. pombe* gene function database 'PomBase'. These proteins are possible targets of mediated effects. Since *tip1*Δ and *ssm4*Δ did not restore growth defects caused by Mal3-overexpression (Fig4-8B), Tip1 and Ssm4 are unlikely to be the target of Mal3.

Because the *alp11* gene is essential for growth, the author was not able to test the loss of functional effect of *alp11* upon Mal3-overexpression. Alp11 remains as a possible target of Mal3 mediated effects.

Previously, the author had shown that the *pka1*Δ strain exhibits the TBZ sensitive phenotype, which can be rescued by overexpression of Mal3 [88]. In the current study, the author identified that growth defects and monopolar spindle formation were abolished by the loss of functional Pka1 in Mal3-overxpressing cells. Monopolar spindle formation of the *cut7* mutant is rescued by deletion of *pkl1* or *klp*2, both of which encode a kinesin-14 family minus-end directed microtubule motor [17,92]. Overexpression of Mal3 elevated monopolar spindle formation, similar to that found in the *cut7* mutant, and the growth defect of the *cut7* mutant is consistently rescued by *mal3* deletion [19]. In the authors findings, deletion of *pka1* and glucose limitation rescued growth inhibition and monopolar spindle formation in Mal3-overexpressing cells and the *cut7-446* mutant. These findings suggest that overexpression of Mal3 might cause inactivation of Cut7, and deletion of *pka1* or glucose limitation might affect inactivation of kinesin-14, Pkl1 and/or Klp2. Since overexpression of Mal3 and the *cut7* mutation result in increased 4C DNA contents and mitotic defects such as the *cut* phenotype or chromosome mis-segregation, some cells likely progress DNA replication without mitotic arrest. It has been shown that loss of functional Pka1 rescued the temperature sensitive phenotype of many *cut* mutants, such as the *cut1-693*, *cut2-364*, *cut4-533*, *cut9-665*, and *cut20-100* mutants [69,71–73]. These results indicate that lowering Pka1 activity has an apparent benefit for mitotic progression during chromosomal segregation. Separase (Cut1) and securin (Cut2) involve chromosomal segregation and the APC/C complex, of which Cut4, Cut9, and Cut20 ensure chromosomal segregation through degradation of Cut2. Cut7 is a kinesine-5 microtubule motor protein involved in spindle formation, and a *cut7-446* mutant, in fact, has a mitotic defect in which cells are separated by the septum before nuclear division that results in a mis-segregated nucleus [13]. Despite this, it remains unclear why loss of functional Pka1 would rescue a defective mitotic phenotype in many *cut* mutants. One of the authors hypotheses is that Pka1 may be involved as a spindle assembly checkpoint to monitor aberrant spindle formation and loss of this function could enable mitotic progression. However, further analysis is required to attribute the actual roles of Pka1 to these phenomena.

The growth and cell cycle of *S. pombe* are affected by medium conditions, specifically the concentration of glucose as a carbon source is important [48]. The author found that glucose limitation restored monopolar spindle formation and growth defects caused by Mal3-overexpression and in the *cut7-446* mutant. Glucose limitation has been shown to re-localize Pom1 to cell sides by severe microtubule destabilization and strongly delays mitosis [93]. For microtubule destabilization, Pka1 activity is required to regulate the microtubule rescue factor CLASP/Cls1/Peg1 under glucose-limiting conditions [93]. Since glucose limitation decreases cAMP levels and Pka1 remains inactivated due to its binding with Cgs1

[41,43], Pka1 inactivation rescued the phenotypes observed in Mal3-overexpressing cells and the *cut7-446* mutant, whereas neither the *tor1* nor the *ssp2* deletion rescued Mal3-overexpressing and the *cut7-446* mutant phenotypes, indicating that the glucose response pathways mediated by Tor1 and Ssp2 are not in charge of microtubule formation. Overexpression of Mal3 (1-241) or Mal3 (Q89R) resulted in severe growth defects and elevated monopolar spindle formation, both in the presence of 2% glucose and in the glucose-limiting conditions (Fig. 4-3 and Fig. 4-6). As these phenotypes were not suppressed by the *pka1* deletion [88], the effect of glucose and the relevance of the Pka1 pathway is consistent.

In conclusion, the results of this study demonstrated that the EB1 domain of Mal3 plays a role in proper spindle formation that is coordinated with binding of the Mal3 CH domain binding to microtubules. The authors findings show a novel function for Pka1, regulating proper spindle formation, in regard to the CH and EB1 domains of Mal3 and to the *cut7-446* mutant.

The author propose that Pka1 regulates bipolar spindle formation during mitosis in addition to the known roles of Pka1 in meiosis, gluconeogenesis, chorological aging, stress response, and proper chromosome segregation in *S. pombe*.

Conclusion

In this thesis, Mal3 was analyzed as a new target of the cAMP/PKA pathway. The results in this study focused on the two proteins, *pka1* and *mal3*, which have a relationship that complements each other's phenotypes of deletion strains, and clarified the relationship by analyzes such as genetics and molecular biology. The results of these two different approaches both indicated that Pka1 regulates microtubule or Mal3 function during mitosis. This control system by Pka1 plays important role for mitotic phase event, such as stable chromosome segregation and bipolar spindle formation. Moreover, since it is suggested that amount of glucose was also involved, cAMP/PKA pathway regulates mitotic phase event. In the *pka1* deletion strain, it is considered that such a control system fails and the microtubule polymerization inhibitor becomes fragile. These findings provide new insight that fluctuations in the extracellular glucose affect microtubule function with microtubule binding protein Mal3 via the cAMP/PKA pathway.

In addition, this study also revealed some important phenotypes for the physiological function of Mal3. It was revealed that the CH domain has a microtubule-stabilizing function and is conserved across species, and that the EB1 domain and C-terminal region have a role in mitosis. These findings could be useful research targets in future Mal3 research.

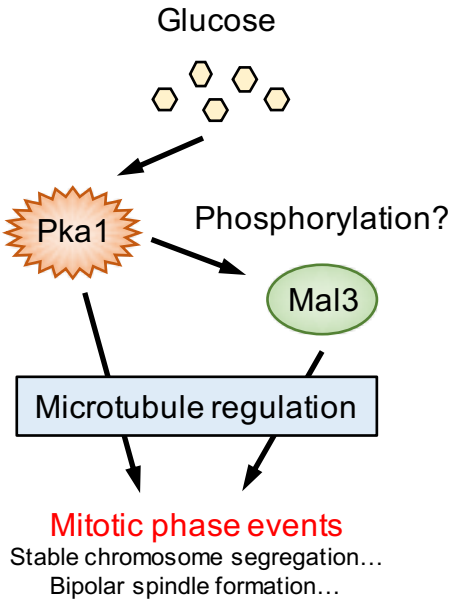

Fig. 4-7. Schematic diagram of summary in this study.

Extracellular glucose affected Pka1 activity. Pka1 regulates through microtubule dynamics, or some targets. Pka1 may phosphorylate Mal3. Mal3 regulate mitotic events through microtubule dynamics or some targets.

Acknowledgments

The author thanks Dr. Kiyosue (RIKEN Center for Life Science Technologies, Japan) for the provision of plasmids pEGFP-N-human EB1 and pGFP-NKB-mouse EB1. The author thanks Dr. Hashimoto and Dr. Hotta (Nara Institute of Science and Technology, Japan) for the provision of plasmids pET32-FHP-ATEB1a, pET32-FHP-ATEB1b, and pET32-FHP-ATEB1c. The author also thanks Drs. M. Iimori (Kyushu University) and T. Matsumoto (Kyoto University) for the provision of anti-Mal3 antibody. FY8144 (MY273), FY10087 (MY2187), and FY13663 (JW952) was provided by the National Bio-Resource Project (NBRP), Japan.

The author would like to express his grateful acknowledgement to his supervisor Professor Makoto Kawamukai, Department of Life Science, Shimane University, For his appropriate advice, English proofreading, valuable suggestions, and encouragement during the course of this work.

The author would like to express his grateful acknowledgement to Associate Professor Yasuhiro Matsuo, Department of Life Science, Shimane University, For his appropriate advice, English proofreading, valuable suggestions, and encouragement during the course of this work.

The author would like to express his grateful acknowledgement to his supervisor Professor Tsuyoshi Nakagawa, Department of Molecular and Functional Genomics, Center for Integrated Research in Science, Shimane University, for his valuable suggestions and encouragement during the course of this work.

The author would like to express his sincere acknowledgement to Associate Professor Tomohiro Kaino, Department of Life Science, Shimane university, for his advices and encouragement during the course of this work

The author would like to express his sincere acknowledgement to Assistant Professor Takushi Hachiya, Department of Molecular and Functional Genomics, Center for Integrated Research in Science, Shimane University, for his valuable suggestions and encouragement during the course of this work.

The author would like to express his sincere acknowledgement to Professor Kinya Akashi, Department of Agricultural, Life and Environmental Sciences, Tottori University, for his advices and encouragement during the course of this work.

The author would like to express his thanks to Mr. Masayuki Yamaga for their experimental supports, and encouragement during the course of this work.

The author would like to express his thanks to Ms. Chikako Yokogi, Dr. Kouhei Nisino, Mr. Tomotake Sakai, Mr. Tomoya Hoshida, Ms. Remi Akagawa, and all other members of Laboratory of Applied Microbiology, Shimane University for their kind supports, technical advices, and encouragement during the course of this study.

References

1. Matthews BJ, Vosshall LB. How to turn an organism into a model organism in 10 “easy” steps. *J Exp Biol.* 2020;223. doi:10.1242/jeb.218198
2. Wood V, Harris MA, McDowall MD, Rutherford K, Vaughan BW, Staines DM, et al. PomBase: A comprehensive online resource for fission yeast. *Nucleic Acids Res.* 2012;40: 695–699. doi:10.1093/nar/gkr853
3. Hayles J, Nurse P. Introduction to fission yeast as a model system. *Cold Spring Harb Protoc.* 2018;2018: 323–333. doi:10.1101/pdb.top079749
4. Cavanaugh AM, Jaspersen SL. Big lessons from little yeast: budding and fission yeast centrosome structure, duplication, and function. *Annu Rev Genet.* 2017;51: 361–383. doi:10.1146/annurev-genet-120116-024733
5. Lansbergen G, Akhmanova A. Microtubule plus end: a hub of cellular activities. *Traffic.* 2006;7: 499–507. doi:10.1111/j.1600-0854.2006.00400.x
6. Akhmanova A, Steinmetz MO. Microtubule +TIPs at a glance. *J Cell Sci.* 2010;123: 3415–3419. doi:10.1242/jcs.062414
7. Toda T, Adachi Y, Hiraoka Y, Yanagida M. Identification of the pleiotropic cell division cycle gene *NDA2* as one of two different α-tubulin genes in *schizosaccharomyces pombe*. *Cell.* 1984;37: 233–242. doi:10.1016/0092-8674(84)90319-2
8. Hiraoka Y, Toda T, Yanagida M. The *NDA3* gene of fission yeast encodes β-tubulin: A cold-sensitive *nda3* mutation reversibly blocks spindle formation and chromosome movement in mitosis. *Cell.* 1984;39: 349–358. doi:10.1016/0092-8674(84)90013-8
9. Stearns T, Evans L, Kirschner M. γ-Tubulin is a highly conserved component of the centrosome. *Cell.* 1991;65: 825–836. doi:10.1016/0092-8674(91)90390-K
10. Horio T, Uzawa S, Jung MK, Oakley BR, Tanaka K, Yanagida M. The fission yeast γ-tubulin is essential for mitosis and is localized at microtubule organizing centres. *J Cell Sci.* 1991;99: 693–700.
11. Miki H, Setou M, Kaneshiro K, Hirokawa N. All kinesin superfamily protein, KIF, genes in mouse and human. *Proc Natl Acad Sci USA.* 2001;98: 7004–7011. doi:10.1073/pnas.111145398
12. Schoch CL, Aist JR, Yoder OC, Turgeon BG. A complete inventory of fungal kinesins in representative filamentous ascomycetes. *Fungal Genet Biol.* 2003;39: 1–15. doi:10.1016/S1087-1845(03)00022-7
13. Hagan I, Yanagida M. Novel potential mitotic motor protein encoded by the fission yeast *cut7*$^{+}$ gene. *Nature.* 1990;347: 563–566. doi:10.1038/347563a0

14. Braun M, Lansky Z, Bajer S, Fink G, Kasprzak AA, Diez S. The human kinesin-14 HSET tracks the tips of growing microtubules in vitro. *Cytoskeleton.* 2013;70: 515–521. doi:10.1002/cm.21133

15. Braun M, Drummond DR, Cross RA, McAinsh AD. The kinesin-14 Klp2 organizes microtubules into parallel bundles by an ATP-dependent sorting mechanism. *Nat Cell Biol.* 2009;11: 724–730. doi:10.1038/ncb1878

16. Troxell CL, Sweezy MA, West RR, Reed KD, Carson BD, Pidoux AL, et al. *pkl1*$^{+}$ and *klp2*$^{+}$: Two kinesins of the Kar3 subfamily in fission yeast perform different functions in both mitosis and meiosis. Mol Biol Cell. 2001;12: 3476–3488. doi:10.1091/mbc.12.11.3476

17. Yukawa M, Yamada Y, Yamauchi T, Toda T. Two spatially distinct kinesin-14 proteins, Pkl1 and Klp2, generate collaborative inward forces against kinesin-5 Cut7 in *S. pombe*. *J Cell Sci.* 2018;131. doi:10.1242/jcs.210740

18. Yukawa M, Teratani Y, Toda T. How Essential Kinesin-5 Becomes non-essential in fission yeast: force balance and microtubule dynamics matter. *Cells.* 2020;9: 1154. doi:10.3390/cells9051154

19. Yukawa M, Yamada Y, Toda T. Suppressor analysis uncovers that maps and microtubule dynamics balance with the Cut7/Kinesin-5 motor for mitotic spindle assembly in *schizosaccharomyces pombe*. *G3 Genes Genomes Genet.* 2019;9: 269–280. doi:10.1534/g3.118.200896

20. Su L, Burrell M, Hill DE, Gyuris J, Brent R, Wiltshire R, et al. APC binds to the novel protein EB1. *Cancer Res.* 1995;55: 2972–2977.

21. Akhmanova A, Steinmetz MO. Tracking the ends: A dynamic protein network controls the fate of microtubule tips. *Nat Rev Mol Cell Biol.* 2008;9: 309–322. doi:10.1038/nrm2369

22. Nehlig A, Molina A, Rodrigues-Ferreira S, Honoré S, Nahmias C. Regulation of end-binding protein EB1 in the control of microtubule dynamics. *Cell Mol Life Sci.* 2017;74: 2381–2393. doi:10.1007/s00018-017-2476-2

23. Beinhauer JD, Hagan IM, Hegemann JH, Fleig U. Ma13, the fission yeast homologue of the human APC-interacting protein EB-1 is required for microtubule integrity and the maintenance of cell form. *J Cell Biol.* 1997;139: 717–728. doi:10.1083/jcb.139.3.717

24. Busch KE, Hayles J, Nurse P, Brunner D. Tea2p kinesin is involved in spatial microtubule organization by transporting Tip1p on microtubules. *Dev Cell.* 2004;6: 831–843. doi:10.1016/j.devcel.2004.05.008

25. Chang F, Martin SG. Shaping fission yeast with microtubules. *Cold Spring Harb Perspect Biol.* 2009;1:a001347. doi:10.1101/cshperspect.a001347

26. Busch KE, Brunner D. The microtubule plus end-tracking proteins mal3p and tip1p cooperate for cell-end targeting of interphase microtubules. Curr Biol. 2004;14: 548–559. doi:10.1016/j.cub.2004.03.029

27. Mana-Capelli S, McLean JR, Chen CT, Gould KL, McCollum D. The kinesin-14 Klp2 is negatively regulated by the SIN for proper spindle elongation and telophase nuclear positioning. *Mol Biol Cell.* 2012;23: 4592–4600. doi:10.1091/mbc.E12-07-0532

28. Kerres A, Vietmeier-Decker C, Ortiz J, Karig I, Beuter C, Hegemann J, et al. The fission yeast kinetochore component Spc7 associates with the EB1 family member Mal3 and is required for kinetochore–spindle association. *Mol Biol Cell.* 2004;15: 5255–5267. doi:10.1091/mbc.e04-06-0443

29. Matsuo Y, Maurer SP, Yukawa M, Zakian S, Singleton MR, Surrey T, et al. An unconventional interaction between Dis1/TOG and Mal3/EB1 promotes the fidelity of chromosome segregation. *J Cell Sci.* 2016; jcs.197533. doi:10.1242/jcs.197533

30. Iimori M, Ozaki K, Chikashige Y, Habu T, Hiraoka Y, Maki T, et al. A mutation of the fission yeast EB1 overcomes negative regulation by phosphorylation and stabilizes microtubules. *Exp Cell Res.* 2012;318: 262–275. doi:10.1016/j.yexcr.2011.11.006

31. Maurer SP, Fourniol FJ, Bohner G, Moores CA, Surrey T. EBs recognize a nucleotide-dependent structural cap at growing microtubule ends. *Cell.* 2012;149: 371–382. doi:10.1016/j.cell.2012.02.049

32. Von Loeffelholz O, Venables NA, Drummond DR, Katsuki M, Cross R, Moores CA. Nucleotide- and Mal3-dependent changes in fission yeast microtubules suggest a structural plasticity view of dynamics. *Nat Commun.* 2017;8: 1–13. doi:10.1038/s41467-017-02241-5

33. Maeda T, Watanabe Y, Kunitomo H, Yamamoto M. Cloning of the *pka1* gene encoding the catalytic subunit of the cAMP- dependent protein kinase in *Schizosaccharomyces pombe*. *J Biol Chem.* 1994;269: 9632–9637.

34. Strutt DI, Wiersdorff V, Mlodzik M. Regulation of furrow progression in the Drosophila eye by cAMP-dependent protein kinase A. *Nature.* 1995;373: 705–709. doi:10.1038/373705a0

35. Taylor SS, Kim C, Cheng CY, Brown SHJ, Wu J, Kannan N. Signaling through cAMP and cAMP-dependent protein kinase: Diverse strategies for drug design. *Biochim Biophys Acta.* 2008;1784: 16–26. doi:10.1016/j.bbapap.2007.10.002

36. Toda T, Cameron S, Sass P, Zoller M, Wigler M. Three different genes in *S. cerevisiae* encode the catalytic subunits of the cAMP-dependent protein kinase. *Cell.* 1987;50: 277–287. doi:10.1016/0092-8674(87)90223-6

37. Kawamukai M, Ferguson K, Wigler M, Young D. Genetic and biochemical analysis of the adenylyl cyclase of *Schizosaccharomyces pombe*. *Mol Biol Cell.* 1991;2: 155–164. doi:10.1091/mbc.2.2.155

38. Kawamukai M, Gerst J, Field J, Riggs M, Rodgers L, Wigler M, et al. Genetic and biochemical analysis of the adenylyl cyclase-associated protein, cap, in *Schizosaccharomyces pombe*. *Mol Biol Cell.* 1992;3: 167–180. doi:10.1091/mbc.3.2.167

39. Matsuo Y, McInnis B, Marcus S. Regulation of the subcellular localization of cyclic AMP-dependent protein kinase in response to physiological stresses and sexual differentiation in the fission yeast *Schizosaccharomyces pombe*. *Eukaryot Cell.* 2008;7: 1450–1459. doi:10.1128/EC.00168-08

40. Welton RM, Hoffman CS. Glucose monitoring in fission yeast via the gpa2 Gα, the git5 Gβ and the git3 putative glucose receptor. *Genetics*. 2000;156: 513–521.

41. Gupta DR, Paul SK, Oowatari Y, Matsuo Y, Kawamukai M. Multistep regulation of protein kinase A in its localization, phosphorylation and binding with a regulatory subunit in fission yeast. *Curr Genet.* 2011;57: 353–365. doi:10.1007/s00294-011-0354-2

42. DeVoti J, Seydoux G, Beach D, McLeod M. Interaction between *ran1*$^{+}$ protein kinase and cAMP dependent protein kinase as negative regulators of fission yeast meiosis. *EMBO J.* 1991;10: 3759–3768. doi:10.1002/j.1460-2075.1991.tb04945.x

43. Byrne SM, Hoffman CS. Six git genes encode a glucose-induced adenylate cyclase activation pathway in the fission yeast *Schizosaccharomyces pombe*. *J Cell Sci.* 1993;105: 1095–1100.

44. Matsuo Y, Kawamukai M. cAMP-dependent protein kinase involves calcium tolerance through the regulation of Prz1 in *Schizosaccharomyces pombe*. *Biosci Biotechnol Biochem.* 2017;81: 231–241. doi:10.1080/09168451.2016.1246171

45. Roux AE, Quissac A, Chartrand P, Ferbeyre G, Rokeach LA. Regulation of chronological aging in *Schizosaccharomyces pombe* by the protein kinases Pka1 and Sck2. *Aging Cell.* 2006;5: 345–357. doi:10.1111/j.1474-9726.2006.00225.x

46. Stiefel J, Wang L, Kelly DA, Janoo RTK, Seitz J, Whitehall SK, et al. Suppressors of an adenylate cyclase deletion in the fission yeast *Schizosaccharomyces pombe*. *Eukaryot Cell.* 2004;3: 610–619. doi:10.1128/EC.3.3.610-619.2004

47. Wu SY, McLeod M. The *sak1*$^{+}$ gene of *Schizosaccharomyces pombe* encodes an RFX family DNA-binding protein that positively regulates cyclic AMP-dependent protein kinase-mediated exit from the mitotic cell cycle. *Mol Cell Biol.* 1995;15: 1479–1488. doi:10.1128/mcb.15.3.1479

48. Petersen J, Russell P. Growth and the environment of *Schizosaccharomyces pombe*. *Cold Spring Harb Protoc.* 2016; 210–226. doi:10.1101/pdb.top079764

49. Murray JM, Watson AT, Carr AM. Transformation of *schizosaccharomyces pombe*: Lithium acetate/dimethyl sulfoxide procedure. *Cold Spring Harb Protoc.* 2016; 394–396. doi:10.1101/pdb.prot090969

50. Takenaka K, Tanabe T, Kawamukai M, Matsuo Y. Overexpression of the transcription factor Rst2 in *Schizosaccharomyces pombe* indicates growth defect, mitotic defects, and microtubule disorder. *Biosci Biotechnol Biochem.* 2018;82: 247–257. doi:10.1080/09168451.2017.1415126

51. Forsburg SL. Comparison of *Schizosaccharomyces pombe* expression systems. *Nucleic Acids Res.* 1993;21: 2955–2956. doi:10.1093/nar/21.12.2955

52. Nakamura S, Grigoriev I, Nogi T, Hamaji T, Cassimeris L, Mimori-Kiyosue Y. Dissecting the nanoscale distributions and functions of microtubule-end-binding proteins EB1 and ch-TOG in interphase HeLa cells. *PLoS One.* 2012;7: 1–20. doi:10.1371/journal.pone.0051442

53. Mimori-Kiyosue Y, Shiina N, Tsukita S. The dynamic behavior of the APC-binding protein EB1 on the distal ends of microtubules. *Curr Biol.* 2000;10: 865–868. doi:10.1016/S0960-9822(00)00600-X

54. Komaki S, Abe T, Coutuer S, Inzé D, Russinova E, Hashimoto T. Nuclear-localized subtype of end-binding 1 protein regulates spindle organization in *Arabidopsis*. *J Cell Sci.* 2010; 123: 451-459 doi:10.1242/jcs.062703

55. Niwa O, Matsumoto T, Yanagida M. Construction of a mini-chromosome by deletion and its mitotic and meiotic behaviour in fission yeast. *MGG Mol Gen Genet.* 1986;203: 397–405. doi:10.1007/BF00422063

56. Matsuo Y, Tanaka K, Nakagawa T, Matsuda H, Kawamukai M. Genetic analysis of *chs1*$^{+}$ and *chs2*$^{+}$ encoding chitin synthases from *Schizosaccharomyces pombe*. *Biosci Biotechnol Biochem.* 2004;68: 1489–1499. doi:10.1271/bbb.68.1489

57. Kanda Y. Investigation of the freely available easy-to-use software "EZR" for medical statistics. *Bone Marrow Transplant.* 2013;48: 452–458. doi:10.1038/bmt.2012.244

58. Davidse LC. BENZIMIDAZOLE FUNGICIDES: MECHANISM OF ACTION AND BIOLOGICAL IMPACT. *Ann Rev Phytopathol.* 1986;24: 43–65.

59. Martin RJ. Modes of action of anthelmintic drugs. *Vet J.* 1997;154: 11–34. doi:10.1016/S1090-0233(05)80005-X

60. He X, Patterson TE, Sazer S. The *Schizosaccharomyces pombe* spindle checkpoint protein mad2p blocks anaphase and genetically interacts with the anaphase-promoting complex. *Proc Natl Acad Sci USA.*1997;94: 7965–7970.

61. Sawin KE, Nurse P. Regulation of cell polarity by microtubules in fission yeast. *J Cell Biol.* 1998;142: 457–471.

62. Hayashi I, Ikura M. Crystal structure of the amino-terminal microtubule-binding domain of end-binding protein 1 (EB1)*. *J Biol Chem.* 2003;278: 36430–36434. doi:10.1074/jbc.M305773200

63. Groot CO De, Jelesarov I, Damberger FF, Scha MA, Bhavesh NS, Grigoriev I, et al. Molecular insights into mammalian end-binding protein. *J Biol Chem.* 2010;285: 5802–5814. doi:10.1074/jbc.M109.068130

64. Asadi F, Michalski D, Karagiannis J. A genetic screen for fission yeast gene deletion mutants exhibiting hypersensitivity to Latrunculin A. *G3: Genes Genomes Genetics.* 2016;6: 3399–3408. doi:10.1534/g3.116.032664

65. Des Georges A, Katsuki M, Drummond DR, Osei M, Cross RA, Amos LA. Mal3, the *Schizosaccharomyces pombe* homolog of EB1, changes the microtubule lattice. *Nat Struct Mol Biol.* 2008;15: 1102–1108. doi:10.1038/nsmb.1482

66. Tallada VA, Daga RR, Palomeque C, Garzón A, Jimenez J. Genome-wide search of *Schizosaccharomyces pombe* genes causing overexpression-mediated cell cycle defects. *Yeast.* 2002;19: 1139–1151. doi:10.1002/yea.902

67. Seung JH, Conti M. New pathways from PKA to the Cdc2/cyclin B complex in oocytes: Wee1B as a potential PKA substrate. *Cell Cycle.* 2006;5: 227–231. doi:10.4161/cc.5.3.2395

68. Mizunuma M, Tsubakiyama R, Ogawa T, Shitamukai A, Kobayashi Y, Inai T, et al. Ras/cAMP-dependent protein kinase (PKA) regulates multiple aspects of cellular events by phosphorylating the whi3 cell cycle regulator in budding yeast. *J Biol Chem.* 2013;288: 10558–10566. doi:10.1074/jbc.M112.402214

69. Kawasaki Y, Nagao K, Nakamura T, Yanagida M. Fission yeast MAP kinase is required for the increased securin-separase interaction that rescues separase mutants under stresses. *Cell Cycle.* 2006;5: 1831–1839. doi:10.4161/cc.5.16.3010

70. Yamada H, Kumada K, Yanagida M. Distinct subunit functions and cell cycle regulated phosphorylation of 2OS APC/cyclosome required for anaphase in fission yeast. *J Cell Sci.* 1997;110: 1793–1804.

71. Yamashita YM, Nakaseko Y, Kumada K, Nakagawa T, Yanagida M. Fission yeast APC/cyclosome subunits, Cut20/Apc4 and Cut23/Apc8, in regulating metaphase-anaphase

progression and cellular stress responses. *Genes to Cells.* 1999;4: 445–463. doi:10.1046/j.1365-2443.1999.00274.x

72. Yamashita YM, Nakaseko Y, Samejima I, Kumada K, Yamada H, Michaelson D, et al. 20S cyclosome complex formation and proteolytic activity inhibited by the cAMP/PKA pathway. *Nature.* 1996;384: 276. Available: http://dx.doi.org/10.1038/384276a0

73. Yanagida M, Yamashita YM, Tatebe H, Ishii K, Kumada K, Nakaseko Y. Control of metaphase-anaphase progression by proteolysis: Cyclosome function regulated by the protein kinase A pathway, ubiquitination and localization. Philos Trans R Soc B Biol Sci. 1999;354: 1559–1570. doi:10.1098/rstb.1999.0499

74. Akera T, Goto Y, Sato M, Yamamoto M, Watanabe Y. Mad1 promotes chromosome congression by anchoring a kinesin motor to the kinetochore. *Nat Cell Biol.* 2015;17: 1124–1133. doi:10.1038/ncb3219

75. Nabeshima K, Kurooka H, Takeuchi M, Kinoshita K, Nakaseko Y, Yanagida M. p93dis1, which is required for sister chromatid separation, is a novel microtubule and spindle pole body-associating protein phosphorylated at the Cdc2 target sites. *Genes Dev.* 1995;9: 1572–1585. doi:10.1101/gad.9.13.1572

76. Snaith HA, Thompson J, Yates JR, Sawin KE. Characterization of Mug33 reveals complementary roles for actin cable-dependent transport and exocyst regulators in fission yeast exocytosis. *J Cell Sci.* 2011;124: 2187–2199. doi:10.1242/jcs.084038

77. Al-Bassam J, Kim H, Flor-Parra I, Lal N, Velji H, Chang F. Fission yeast Alp14 is a dose-dependent plus end-tracking microtubule polymerase. *Mol Biol Cell.* 2012;23: 2878–2890. doi:10.1091/mbc.E12-03-0205

78. Gimona M, Djinovic-Carugo K, Kranewitter WJ, Winder SJ. Functional plasticity of CH domains. *FEBS Lett.* 2002;513: 98–106. doi:10.1016/S0014-5793(01)03240-9

79. Blangy A, Lane HA, d'Hérin P, Harper M, Kress M, Niggt EA. Phosphorylation by p34cdc2 regulates spindle association of human Eg5, a kinesin-related motor essential for bipolar spindle formation in vivo. *Cell.* 1995;83: 1159–1169. doi:10.1016/0092-8674(95)90142-6

80. Enos AP, Morris NR. Mutation of a gene that encodes a kinesin-like protein blocks nuclear division in A. nidulans. *Cell.* 1990;60: 1019–1027. doi:10.1016/0092-8674(90)90350-N

81. Goshima G, Vale RD. The roles of microtubule-based motor proteins in mitosis: Comprehensive RNAi analysis in the Drosophila S2 cell line. *J Cell Biol.* 2003;162: 1003–1016. doi:10.1083/jcb.200303022

82. Hoyt MA, He L, Kek Khee Loo, Saunders WS. Two *Saccharomyces cerevisiae* kinesin-related gene products required for mitotic spindle assembly. *J Cell Biol.* 1992;118: 109–120. doi:10.1083/jcb.118.1.109

83. Mann BJ, Wadsworth P. Kinesin-5 Regulation and Function in Mitosis. *Trends Cell Biol.* 2019;29: 66–79. doi:10.1016/j.tcb.2018.08.004

84. Hoffman CS. Glucose sensing via the protein kinase A pathway in *Schizosaccharomyces pombe*. *Biochem Soc Trans.* 2005;33: 257–260. doi:10.1042/BST0330257

85. Kim JH, Roy A, Jouandot D, Cho KH. The glucose signaling network in yeast. *Biochim Biophys Acta - Gen Subj.* 2013;1830: 5204–5210. doi:10.1016/j.bbagen.2013.07.025

86. Santangelo GM. Glucose signaling in *Saccharomyces cerevisiae*. *Microbiol Mol Biol Rev.* 2006;70: 253–282. doi:10.1128/MMBR.70.1.253

87. Van Ende M, Wijnants S, Van Dijck P. Sugar sensing and signaling in *Candida albicans* and *Candida glabrata*. *Front Microbiol.* 2019;10: 1–16. doi:10.3389/fmicb.2019.00099

88. Tanabe T, Yamaga M, Kawamukai M, Matsuo Y. Mal3 is a multi-copy suppressor of the sensitivity to microtubule-depolymerizing drugs and chromosome mis-segregation in a fission yeast *pka1* mutant. *PLoS One.* 2019;14: 1–24. doi:10.1371/journal.pone.0214803

89. Gupta DR, Paul SK, Oowatari Y, Matsuo Y, Kawamukai M. Complex formation, phosphorylation, and localization of protein kinase A of *schizosaccharomyces pombe* upon glucose starvation. *Biosci Biotechnol Biochem.* 2011;75: 1456–1465. doi:10.1271/bbb.110125

90. Matsuzawa T, Fujita Y, Tohda H, Takegawa K. Snf1-like protein kinase *ssp2* regulates glucose derepression in *schizosaccharomyces pombe*. *Eukaryot Cell*. 2012;11: 159–167. doi:10.1128/EC.05268-11

91. Saitoh S, Mori A, Uehara L, Masuda F, Soejima S, Yanagida M. Mechanisms of expression and translocation of major fission yeast glucose transporters regulated by CaMKK/phosphatases, nuclear shuttling, and TOR. Mol Biol Cell. 2015;26: 373–386. doi:10.1091/mbc.E14-11-1503

92. Yukawa M, Kawakami T, Okazaki M, Kume K, Tang NH, Toda T. A microtubule polymerase cooperates with the kinesin-6 motor and a microtubule cross-linker to promote bipolar spindle assembly in the absence of kinesin-5 and kinesin-14 in fission yeast. *Mol Biol Cell.* 2017;28: 3647–3659. doi:10.1091/mbc.E17-08-0497

93. Kelkar M, Martin SG. PKA antagonizes CLASP-dependent microtubule stabilization to re-localize Pom1 and buffer cell size upon glucose limitation. *Nat Commun.* 2015;6. doi:10.1038/ncomms9445

Summary

Fission yeast needs to adapt rapidly to any changes in the extracellular environments, and the responsive pathways for these have been studied by many researchers as a model of unicellular organism. The recognition of glucose, which is a major carbon source, is essential for survival for the living cells to alter metabolism depending on its availability. The carbon source response involves several types of signal transduction pathways, among which the cAMP/protein kinase A (PKA) pathway is a major one and widely conserved from yeasts to humans.

The cAMP/PKA pathway in fission yeast is involved in gluconeogenesis, transition from mitosis to meiosis, stress response and etc. However, other than these cellular responses, not so much functions have been unveiled, and only a few targets for PKA have been identified. On the other hand, it has been known that the loss of functional PKA (by *pka1* deletion) results in sensitivity to various drugs such as $CaCl_2$, microtubule polymerization inhibitors (mitotic phase inhibitors), and DNA replication inhibitors. For this reason, it is expected that multiple unclear regulatory systems may exist in the downstream of PKA.

The laboratory the author belonging to has been focused on the sensitivity by microtubule polymerization inhibitor in *pka1* deletion strains, and the authors collaborator isolated *mal3* as a multi-copy suppressor which reversed the TBZ sensitive phenotype of the *pka1*Δ strains. Mal3 is a microtubule-binding protein classified in a type of the EB1 family proteins. Mal3 consists of two domains designated the CH and EB1 domains. The CH domain is a microtubule-binding domain, and the EB1 domain, which is highly conserved in EB1 family proteins, involves morphogenesis and chromosome distribution. The author conducted a study to clarify the cause of sensitivity to microtubule polymerization inhibitor in *pka1* deletion strains and to clarify a new regulatory system by PKA in conjunction with Mal3.

First, the author analyzed the phenotype of *pka1* deletion strains to microtubule polymerization inhibitors. Since microtubule polymerization inhibitors such as TBZ act during mitosis, DAPI staining and chromosome segregation analysis were conducted. As a result, in the presence of TBZ, the *pka1* deletion strain had a significantly increased frequency of abnormal chromosome segregation compared to the wild-type strain. Since the *mal3* deletion strain exhibited microtubule polymerization inhibitor sensitivity, the sensitivity of a double deletion strain of *mal3* and *pka1* was tested by spot assay. The result showed the sensitivity became stronger than each single deletion strain. This suggests that the sensitivity of individual *pka1* and *mal3* deletion strain is caused by a different factor. The author then fragmented Mal3 into two domains, and each was expressed in a *pka1* deletion strain. Then, the suppression of microtubule polymerization inhibitor

sensitivity and the function of each domain of Mal3 was investigated. As a result, the sensitivity was suppressed only by expression of the CH domain, which has at least the functions of microtubule binding and microtubule stabilization. The author further analyzed several mutants that affect the ability of the CH domain to bind to microtubules. As a result, the suppression ability depended on the ability of Mal3 to bind to microtubules. In addition, the author analyzed whether this function was conserved in other species and in fact it was conserved in most species. Thus, the microtubule-stabilizing function of the CH domain is critical for the suppression of sensitivity to microtubule polymerization inhibitor by Mal3 overexpression in *pka1* deletion strains.

Next, the author analyzed the possibility that Pka1 might affect Mal3 function. Overexpression of Mal3 causes growth inhibition accompanied by monopolar spindle formation during mitosis. The author attempted to elucidate the function of Mal3 during mitosis by analyzing precisely this phenotype. As a result of analysis using fragmentation and mutants of Mal3, the author observed that growth inhibition by Mal3 was caused by both the microtubule-binding ability of the CH domain and the EB1 domain. The monopolar spindle formation caused by Mal3 overexpression was suppressed in the *pka1* deletion strain. It has been known that glucose limitation causes a down regulation of the cAMP/PKA pathway. Therefore, the author analyzed if glucose limitation also suppressed the phenotype observed in the *pka1* deletion strain. Since the phenotype caused by high expression of Mal3 was similarly observed in the *cut7-446* mutant, the author examined and found that phenotypes in *cut7-446* was suppressed by *pka1* deletion and glucose limitation. These results suggest that *pka1* deletion strains and glucose limitation regulate mitotic progression via Mal3 or microtubule regulation.

The results of the present study by these two different approaches indicate that Pka1 regulates microtubule or Mal3 function during mitosis, and also contributes to the weakness of *pka1* deletion strains to microtubule polymerization inhibitors. These findings propose a new mechanism of that extracellular glucose level which is transmitted to the cAMP/PKA pathway affect microtubule function through the microtubule-binding protein Mal3 and else.

List of publications

Chapter 3

Takuma Tanabe, Masayuki Yamaga, Makoto Kawamukai, and Yasuhiro Matsuo (2019)

Mal3 is a multi-copy suppressor of the sensitivity to microtubule-depolymerizing drugs and chromos ome mis-segregation in a fission yeast *pka1* mutant

PLoS ONE 14(4): e0214803

Chapter 4

Takuma Tanabe, Makoto Kawamukai, and Yasuhiro Matsuo (2020)

Glucose limitation and *pka1* deletion rescue aberrant mitotic spindle formation induced by Mal3 overexpression in *Schizosaccharomyces pombe*

Bioscience, Biotechnology, and Biochemistry, 84 (8), 1667-1680, 2020

要旨

単細胞のモデル生物である分裂酵母は、細胞外の環境の変化に対して素早く適応する必要があり、そのための応答経路の研究が盛んに行われてきた。主要な炭素源であるグルコースの認識は、生命維持にとって必要不可欠であり、その存在量に応じて生体内に様々な代謝変化を引き起こす。炭素源の応答は、数種類のシグナル伝達経路が関与するが、なかでも cAMP/プロテインキナーゼ A(PKA)経路が主要な経路であり、酵母からヒトまで広く保存されている。

分裂酵母における cAMP/PKA 経路は、糖新生、有性生殖過程への移行、ストレス応答などに関与する。しかしながら、これまでの研究では、糖新生と有性生殖過程への移行以外の生体内機能はあまり明らかになっておらず、PKA の標的因子はほとんど同定されていない。一方で、PKA 機能欠損株(*pka1* 欠損株)は、塩化カルシウム、微小管重合阻害剤(有糸分裂期阻害剤)、DNA 合成阻害剤などに感受性を示すことがわかっている。これらの事実から、PKA の下流には、明らかになっていない制御系が複数存在することが予想される。

我々の研究グループでは、*pka1* 欠損株が示す微小管重合阻害剤感受性に着目し、この原因を明らかにするための 1 つのアプローチとして、前任者によってマルチコピーサプレッサーの単離が行われた。その結果、1 つの候補として EB1 ファミリータンパク質 Mal3 が単離された。Mal3 は微小管結合タンパク質であり、微小管結合ドメインである CH ドメインと EB1 ファミリータンパク質に高く保存されている EB1 ドメインという 2 つのドメインから成り、形態形成や染色体分配に関与する。私は、Pka1 と Mal3 の関連性の解析を切り口として、*pka1* 欠損株の微小管重合阻害剤感受性の原因を解明するとともに、PKA の新たな制御系を明らかにすることを目的として研究を行なった。

初めに、*pka1* 欠損株の微小管重合阻害剤に対する表現型について解析を行なった。微小管重合阻害剤は有糸分裂期において作用するため、DAPI 染色と染色体分配の解析を行った。その結果、微小管重合阻害剤存在下において、*pka1* 欠損株は野生株と比較して、有意に染色体分配異常の頻度が増加した。また、*mal3* 欠損株においても微小管重合阻害剤感受性を示すため、*pka1* 欠損株との二重破壊株を作成し、スポットテストを行なった。その結果、それぞれの単独破壊株よりも感受性が強くなった。このことから、*pka1* と *mal3* のそれぞれの欠損による感受性は異なる要因によって起こることが示唆された。次に、Mal3 を 2 つのドメイン毎に断片化し、*pka1* 欠損株にそれぞれを発現させ、微小管重合阻害剤感受性の抑圧が引き起こされるか解析し、Mal3 のそれぞれのドメインの関与について調べることにした。その結果、微小管結合と微小管安定化の機能をもつ CH ドメインを含む断片においてのみ、感受性を抑圧した。そこで、CH ドメインの微小管結合能に影響を与えるいくつかの変異体を解析した結果、この抑圧能は Mal3 の微小管結合能に依存していることがわかった。また、この機能が他の生物種で保存されているかを調べたところ、ほとんどの生物種においてこの機能が保存されていた。これ

らの結果から、*pka1* 欠損株の Mal3 による微小管重合阻害剤感受性の抑圧は、CH ドメインの持つ微小管安定化機能によって引き起こされていることが示唆された。

次に、逆のアプローチとして、Pka1 が Mal3 機能に影響を与える可能性について解析した。Mal3 の過剰発現は、有糸分裂期における単極性紡錘体形成を伴う生育阻害が引き起こされる。この表現型を解析して、有糸分裂期における Mal3 機能の解明を試みた。初めに、断片化や変異体を用いた解析の結果、Mal3 による生育阻害は CH ドメインの微小管結合能と EB1 ドメインの両方が存在することで引き起こされていた。また、この単極性紡錘体形成は、*pka1* 欠損株で抑圧された。グルコースを制限することは Pka1 経路の機能低下を引き起こす。そのため、グルコース制限下でも解析したところ、*pka1* 欠損株と同様に表現型を抑圧していた。Mal3 高発現によって起こる表現型は *cut7-446* 変異体でも見られるため、同様の解析を行ったところ、*pka1* 欠損株とグルコース制限下で抑圧された。これらのことから、*pka1* 欠損株およびグルコース制限は、Mal3 もしくは微小管制御を介して、有糸分裂期進行を制御していることが示唆された。

これら 2 つの異なるアプローチの研究結果は、どちらも有糸分裂期において Pka1 が微小管もしくは Mal3 機能を制御していることを示しており、*pka1* 欠損株の微小管重合阻害剤に対する脆弱性の要因もこれによるものであることが考えられる。これらの発見は、細胞外グルコース量の変動が、cAMP/PKA 経路を介して、微小管結合タンパク質 Mal3 と共に微小管機能に影響を与えるという新たな知見を示すものである。